LBNL-1005092

ERNEST ORLANDO LAWRENCE
BERKELEY NATIONAL LABORATORY

Balancing daylight, glare, and energy-efficiency goals: An evaluation of exterior coplanar shading systems using complex fenestration modeling tools

Sabine Hoffmann, Eleanor S. Lee, Andrew McNeil, Luis Fernandes, Dragan Vidanovic, Anothai Thanachareonkit

Energy Technologies Area
November 2015

Energy and Buildings 112 (2016): 279-298
doi:10.1016/j.enbuild.2015.12.009

Disclaimer

This document was prepared as an account of work sponsored by the United States Government. While this document is believed to contain correct information, neither the United States Government nor any agency thereof, nor The Regents of the University of California, nor any of their employees, makes any warranty, express or implied, or assumes any legal responsibility for the accuracy, completeness, or usefulness of any information, apparatus, product, or process disclosed, or represents that its use would not infringe privately owned rights. Reference herein to any specific commercial product, process, or service by its trade name, trademark, manufacturer, or otherwise, does not necessarily constitute or imply its endorsement, recommendation, or favoring by the United States Government or any agency thereof, or The Regents of the University of California. The views and opinions of authors expressed herein do not necessarily state or reflect those of the United States Government or any agency thereof or The Regents of the University of California.

Acknowledgment

This work was supported by the Assistant Secretary for Energy Efficiency and Renewable Energy of the U.S. Department of Energy under Contract No. DE-AC02-05CH11231.

This work was supported by the California Energy Commission through its Public Interest Energy Research (PIER) Program on behalf of the citizens of California.

Completion of the paper was supported through the research center High Performance Composite Constructions, HiPerCon, at University of Kaiserslautern.

Balancing daylight, glare, and energy-efficiency goals: an evaluation of exterior coplanar shading systems using complex fenestration modeling tools

Sabine Hoffmann[1], Eleanor S. Lee, Andrew McNeil, Lúis Fernandes, Dragan Vidanovic, Anothai Thanachareonkit.

Building Technology and Urban Systems Division, Energy Technologies Area, Lawrence Berkeley National Laboratory, Mailstop 90-3111, 1 Cyclotron Road, Berkeley, CA 94720 USA

Abstract

Exterior shades are the most effective way to control solar load in buildings. Twelve different coplanar shades with different geometry, material properties and cut-off angles were investigated for two California climates: the moderate San Francisco Bay Area climate and a hot and dry Southern California climate. The presented results distinguish themselves from other simulation studies by a newly developed method that combines three research-grade software programs (Radiance, EnergyPlus and Window 7) to calculate heat transfer, daylight, and glare resulting from optically-complex fenestration systems more accurately. Simulations were run for a case with constant electric lighting and a case with daylighting controls for a prototypical, internal load dominated office building.

In the case of daylighting controls, the choice of slat angle and solar cut-off angle of a fixed exterior slat shading system is non trivial. An optimum slat angle was identified for the considered cases. Material properties (e.g., solar and visible reflectance) did not affect energy use if constant electric lighting was assumed, but they did have a significant influence on energy use intensity (EUI) when daylighting controls were assumed. Energy use increased substantially when an additional interior shade was used for glare control.

Keywords: Exterior shades, Energy Use Intensity, EnergyPlus, Radiance, Complex Fenestration Systems, Glare Control, Discomfort Glare

[1] Corresponding author, Tel.: +49 631 205 2909. E-mail address: Sabine.Hoffmann@bauing.uni-kl.de.

1. Introduction

In the attempt to save energy in commercial buildings, exterior shades are more and more frequently seen in new construction projects in California, the US, and worldwide, and entire architectural trends are formed around the need to reduce solar load in the perimeter zones of high-rise buildings. Exterior shades, compared to other types of shading devices such as interior shades, between-pane shades or compared to electro-chromic glazing, are the most efficient way to reduce solar load because they block a large percentage of direct radiation before it hits the building envelope.

Solar radiation can be very beneficial, for example at times when heating energy is needed. In office buildings, a significant benefit can be achieved by the visible light from the sun if there is a controlled lighting system installed which dims the electric lighting whenever the required illuminance level in the room can be fully or partially met by daylight ("daylighting control"). Therefore, blocking the sun means a trade-off between heating, cooling, fan and lighting energy which has to be considered when making the decision for an exterior shade.

While there are established standards (e.g. NFRC [1]) and metrics (e.g. SHGC[2]) to determine the performance of glazing systems with various substrates and coatings, there are only few simple methods available to classify external shading systems such as EN 13363 [2] which calculates an overall solar heat gain coefficient for slat shading systems including the glazing system. Classifying exterior shades is challenging because of their two- or three-dimensional geometry. Depending on the sun angle, the transmitted radiation and the heat transfer through a complex fenestration system (CFS) varies significantly over the course of the day and the course of the year.

The section for non-residential buildings in Title 24 [3], the mandatory energy-efficiency standard for new constructions in California, requires in its prescriptive approach a RSHGC[3] value for the whole window (including frame and potential window reveals) of 0.25 for fixed windows, 0.22 for operable windows, and 0.26 for curtain walls. The prescriptive approach of Title 24 defines a glazing system to be code compliant if it is combined with "an exterior operable shading louver or other exterior shading device that meets the required SHGC" or "a combination of Items A (glazing system) and B (exterior shading) to achieve the same performance" [3]. However, Title 24 does not provide a calculation method of RSHGC for windows with external shading devices other than overhangs and fins.

The prescriptive method is only applicable to buildings with a window-to-wall ratio (WWR) ≤ 40 %. For WWRs greater than 40 % the alternative calculation method (ACM) with a compliant building simulation software program has to be used. Similar to the prescriptive approach, Title 24 compliant software for proof of code compliance of the building does not necessarily provide the capability of modeling exterior shades other than overhangs and fins.

The accurate modeling of exterior shading devices and their impact on energy performance of a building requires a detailed representation of the geometric model in the simulation, the knowledge of the material surface properties (short-wave and long-wave reflectance, transmittance, absorptance / emittance), and the necessary simulation tools to calculate angle-dependent properties of the system and their impact on energy performance of the building. The aim of this work is therefore manifold: 1) evaluate the potential of energy savings through exterior shades for large office buildings in California, 2) assess the variance of performance by modeling a variety of exterior shading systems which represent current practice in new construction and

[2] SHGC: solar heat gain coefficient. SHGC defines the percentage of incident radiation which penetrates the interior space through the fenestration system either as transmitted radiation or as heat flux.
[3] RSHGC: area-weighted average Relative Solar Heat Gain Coefficient according to Title 24. RSHGC includes frame and glazing area, and is modified if overhangs or fins are present

retrofit, and 3) gain insight as to which class of exterior shading system is preferable for a certain window-to-wall ratio and for specific climates.

While most building energy simulation programs have some capability of modeling blinds or simple shade geometries, the presented results distinguish themselves from previous studies by the selection of the modeling tools used and the subsequent accuracy of the results. Furthermore it considers a long neglected aspect in the trade-offs related to exterior shades which is especially important in office buildings and which has been excluded from building energy analysis for a long time: the occurrence of glare and the necessity to deploy an additional interior shade for glare control under certain conditions.

If office employees at work stations are disrupted in their work by high luminance levels from the façade, they are likely to lower the interior shade to reduce discomfort glare at their desks. Interior shades are only moderately efficient in reducing solar load because they block radiation only after it has entered the indoor space, but they reduce the availability of daylight significantly. The reduction of glare is the primary purpose when using interior shades. Unfortunately, however, interior shades often remain deployed after the glare condition has been resolved, and the deployed shades keep reducing daylight availability and the benefit of daylighting controls.

2. Methods

2.1. Characterization of the complex fenestration systems

The twelve exterior shading systems assessed in this study were chosen to represent a wide range of exterior shades and materials used in modern architecture as well as in retrofit projects. The combination of shading system and glazing system is called complex fenestration system (CFS) in the following sections.

2.1.1. Properties of the reference glazing and interior shade

The base window system is defined as an argon-filled dual-pane window with an outboard layer of low-iron glass, a low-e coating (e = 0.018) on surface two that is spectrally selective, and an inboard layer of clear glass (system thickness: 24 mm). The center-of-glass (COG) U-value of the dual-pane insulating glass unit is 1.4 $W/(m^2K)$, the solar heat gain coefficient is 0.30, and the visible transmittance is 0.65 (Table 1). Assuming a frame-to-window ratio of 15 %, the chosen base window would fulfill the prescriptive requirements of the California code requirements described in Title 24 [3] for curtain walls, which represent the most common type of facade for modern large office buildings with large glazed areas. For reference, in addition to the complex fenestration systems, all simulations were also run with the base window only.

In section 4 the base window and the test cases were modeled with an indoor, light gray (R_{sol} = 0.75) fabric roller shade with an openness factor of 3 % and diffusing properties to reduce discomfort glare. The solar-optical properties of the shade were measured using a goniophotometer, similar to some of the exterior shading systems described below. Performance values of the base window and the test cases with and without interior shade can be found in Table 1.

2.1.2. Description of the exterior shading systems

The range of modeled exterior shading systems comprises slat shading systems, louvers, meshes and external roller shades. All systems were modeled without mounts or anchors, with no connection to the window and at a distance to the outer glass layer which is representative for the class of system. Opening factors according to ISO 15099 [4] account for the air flow between exterior shade and glazing systems. The long-wave emittance of the slat shading systems was calculated based on integrated hemispherical reflectance of the system using

the emissivity of the slat material. The emittance of the meshes was measured and the emittance of the interior roller shade was estimated based on material emissivity and front opening factor. Shade conductance was calculated as a weighted average of material conductivity and thermal conductivity of air, using the front opening multiplier as weighting factor. The performance values of the exterior shading systems can be found in Table 1, the material properties and simulation input values can be found in Table 2a, 2b, and 2c. The geometry of the exterior shades is shown in Appendix B.

BASE GLAZING SYSTEM AND COMPLEX FENESTRATION SYSTEMS						
Name	Without interior shade			With interior shade		
	U-value [W/m^{2}K] COG	Solar Heat Gain Coefficient	Visible Transmittance T_{vis}	U-value [W/m^{2}K] COG	Solar Heat Gain Coefficient	Visible Transmittance T_{vis}
base glaz.	1.4	0.30	0.65	1.2	0.17	0.09
shd 1	1.1	0.31	0.63	1.0	0.19	0.09
shd 2	1.1	0.18	0.34	0.9	0.11	0.05
shd 3	1.0	0.07	0.10	0.9	0.05	0.01
shd 4	1.1	0.05	0.06	0.9	0.04	0.01
shd 5	1.0	0.03	0.03	0.9	0.03	0.00
shd 6	1.0	0.08	0.12	1.0	0.07	0.02
shd 7a	1.0	0.10	0.18	1.0	0.08	0.07
shd 7b	1.0	0.09	0.12	1.0	0.09	0.02
shd 7c	1.0	0.09	0.13	1.0	0.08	0.03
shd 8	1.1	0.14	0.27	1.1	0.12	0.02
shd 9	1.0	0.10	0.17	1.0	0.08	0.05
shd 10	1.0	0.18	0.34	0.9	0.12	0.05

Table1: Performance values for base glazing and CFS based on Window7 calculations. All values are for the center of glass (COG).

2.1.2.1 Window screens – micro slat shading systems (shd 1 – 5)

Shd 1 – 5 are variations of a commercial window screen product [5] that is mainly used in retrofit projects. It attaches to the frame or to a separate support, and is usually mounted close to the window although it could be used at a greater distance to the façade as well. The screens are slat shading systems at a micro scale. Slat angles and the solar cut-off angles[4] were varied by changing the ratio of width and spacing.

The advantage of this type of exterior shading systems is its low weight which reduces installation cost compared to heavier slat shading systems. As the added structural load is negligible the screens are a good option for retrofit. Because of their microstructure the screens allow for a view to the outside. Drawbacks are aesthetic ones as the screen changes the appearance of the building, and the shading system may impair the window cleaning unless it is removable.

2.1.2.2 Retractable and adjustable exterior shades (shd 6 – 7)

Shd 6 is an external roller shade made of stainless steel that rolls up into a casing on the window head powered by an electric motor [6]. The motor can be automated through control software or activated manually. It can be fully or partially retracted and allows therefore better control over solar radiation, daylight and glare. The lateral guard rail in which the roller shade moves secures it against wind loads and acts as an additional vertical shading fin.

[4] Cut-off angle: lowest profile angle at which the system still allows direct radiation – see also Appendix B

Shd 7 is a retractable exterior shade including casing and guard rails with the additional option of adjusting the slat angle either manually or automated [7]. Depending on the width of the system the manufacturer guarantees a safe use of the deployed shade up to wind speeds of 15 – 22 m/s, which makes the product suitable for high rise buildings. At wind speeds that exceed the recommended value the shade should be retracted. The manufacturing company offers a broad selection of finishes with different optical properties. Three variations were considered in this study: a highly reflective finish (shd 7a)[5], a finish with low reflectance (shd 7b), and a finish that is promoted as being selective, i.e. a higher reflectance in the visible spectrum than over the entire solar spectrum (shd 7c) (see Table 2c).

The external roller shade and the retractable, adjustable slat shading system are more elaborate technologies, but also pricier than a fixed slat system. As with every motorized device, the risk of failure and subsequent need of replacement of movable parts raise the maintenance cost. Both retractable shades were modeled as non-operable, static, fully lowered exterior shading systems in this study.

2.1.2.3 Aluminum louvers – macro slat shading systems (shd 8)

Shd 8 represents a common choice for fixed exterior shades: an oval shaped extruded aluminum louver that can be manufactured in any size and length and mounted at any horizontal or vertical angle and with any spacing between louvers. Aluminum louvers are most frequently used in up to five-story-buildings as their size and weight makes them susceptible to wind loads. In addition to macro scale, hollow aluminum can also be found as inserts into shutters and sliding shades.

The variability of shape and size allows architects and engineers to optimize for design and/or performance and the breadth of possible manufacturers can help reduce cost. Attaching the support system for large louvers to the building requires special attention to avoid significant thermal bridges. The relatively high reflectance of aluminum (~ 0.7) will decrease over time with exposure to climate and dirt, and cleaning the louvers can prove challenging and/or cost-intensive. The considered shd 8 was modeled at a 45 deg angle from horizontal (lower edge of slat facing the outdoors) with a solar cut-off vertical angle of 30 deg.

2.1.2.4 Meshes and perforated metal sheets (shd 9 – 10)

Over the past 10 years the use of metal meshes on commercial or institutional buildings emerged as a new architectural trend. Metal meshes offer probably the largest range of products with almost any finish, geometry and opening factor possible. Perforated metal sheets with various perforation patterns are part of this class of fixed exterior shades which are usually used at a greater distance to the façade than most other exterior shades and which cover large parts of the building.

In addition to a specific metal mesh (shd 10) that is distributed in various shading applications [8], a less frequent polymer mesh (shd 9) [9] which is used in a similar way as the metal mesh has been modeled as well. The optical properties of both meshes were measured at the Lawrence Berkeley National Laboratory (LBNL) as their filigree structure makes geometrical CAD modeling difficult.

[5] Due to pollution, the high reflectance values of shd 7a cannot be maintained under outside conditions. Shd 7a is therefore mainly of theoretical interest.

West London County Court, England
Micro-shade attached to windows (shd2)

(picture: Courtesy of smartlouvre)

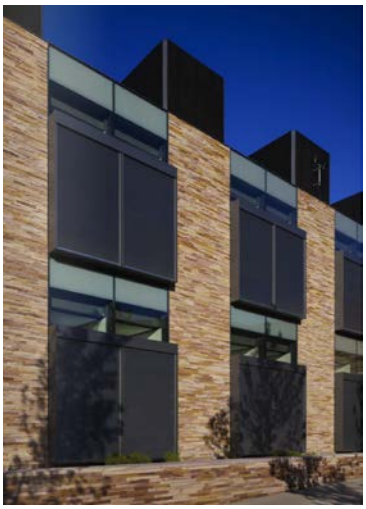

Hilton Foundation, Agoura Hills, USA
Stainless steel roller shade (shd 6)

(picture: Courtesy of ZGF Architects, LLP; Photograph Nick Merrick © Hedrich Blessing)

Center for elderly people, Switzerland
Curved blinds in roller shade (shd 7)

(picture: Courtesy of Warema)

Li Ka Shing, UC Berkeley campus, USA
Aluminum louvers above operable windows and in shutters (similar to shd 8)

(picture: Courtesy of ZGF Architects, LLP; © Robert Canfield)

Museo delle Scienze-Trento , Italy

Fabric mesh (shd 9)

(picture: Serge Ferrari © Andrea Liverani)

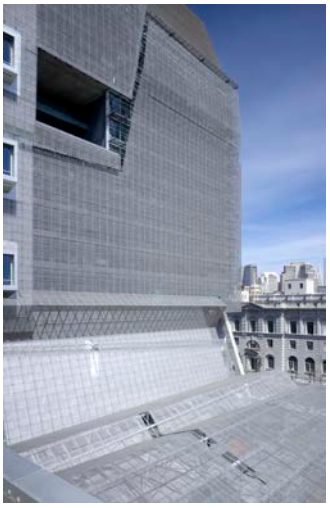

Federal Building San Francisco , USA
Metal mesh (similar to shd 10)

(picture: Courtesy of Tim Griffith; © Tim Griffith)

Fig. 1: Examples of exterior shades

Name	Distance from glass [mm]	Thickness of system [mm]	Material Conductivity [W/mK]	Shade Conductance [W/mK]	Front Opening Multiplier [-]	Cut-off angle [deg]
INTERIOR SHADE						
Interior Shade	50	1.0	0.15	0.15	0.03	n.a.
EXTERIOR SHADE						
shd 1	13	1.3	15	0.17	0.99	45
shd 2	13	1.1	15	2.12	0.86	30
shd 3	13	0.6	15	7.51	0.50	15
shd 4	13	2.5	15	2.12	0.86	0
shd 5	13	0.5	15	7.51	0.50	0
shd 6	50	4.0	15	11.6	0.23	20
shd 7a, 7b, 7c	50	42	150	46.5	0.69	30
shd 8	50	42	150	46.5	0.69	30
shd 9	500	1.0	(0.20)	0.15	0.28	n.a.
shd 10	500	5.0	(0.65)	20	0.40	n.a.

Table2a: Properties of the shading systems and simulation input values

Name	IR Trans-mittance [-]	Material Emissivity [-] x	Shade Emittance [-]	Top Opening Multiplier [-]	Right/Left Opening Multiplier [-]	Bottom Opening Multiplier [-]
INTERIOR SHADE						
Interior Shade	0.03	0.9	0.873	0	0.5	0.5
EXTERIOR SHADE						
shd 1	0.52	0.5	0.37	0	0	0
shd 2	0.45	0.5	0.38	0	0	0
shd 3	0.27	0.5	0.43	0	0	0
shd 4	0.26	0.5	0.55	0	0	0
shd 5	0.27	0.5	0.43	0	0	0
shd 6	0.23	0.6	0.46	0.25	0.50	0.50
shd 7a	0.50	0.1	0.085	0.25	1.0	1.0
shd 7b, 7c	0.41	0.5	0.38	0.25	1.0	1.0
shd 8	0.50	0.1	0.085	1.0	1.0	1.0
shd 9	0.29	-	0.29	0.25	0.25	0.25
shd 10	0.371	-	0.114	0.25	0.25	0.25

Table2b: Properties of the shading systems and simulation input values

Name	Diffuse Solar Reflectance [-]	Total Solar Reflectance [-]	Diffuse Visible Reflectance [-]	Total Visible Reflectance [-]
INTERIOR SHADE				
Interior Shade*	0.75	0.75	0.75	0.75
EXTERIOR SHADE				
shd 1	0.50	0.50	0.50	0.50
shd 2	0.50	0.50	0.50	0.50
shd 3	0.50	0.50	0.50	0.50
shd 4	0.50	0.50	0.50	0.50
shd 5	0.50	0.50	0.50	0.50
Shd 6	0.40	0.55	0.41	0.60
shd 7a	0.87	0.87	0.93	0.93
shd 7b	0.08	0.08	0.15	0.15
shd 7c	0.56	0.56	0.40	0.40
shd 8	0.70	0.70	0.70	0.70
shd 9*	0.30	0.30	0.30	0.30
shd 10*	0.38	0.38	0.38	0.38

*Table2c: Material reflectance (*shade reflectance)*

2.1.3. Thermal and optical properties of the complex fenestration systems

As simulation results are very sensitive to optical properties and moderately sensitive to thermal properties, a lot of care was given to the calculation or measurement of these values. The optical properties of complex fenestration systems depend on the incidence angle of the solar radiation. Therefore the geometries of shades 1 – 8 were modeled with Sketchup (for geometries and dimensions see Appendix B), and the Radiance module *genbsdf* [10] was then used to describe the geometry of the shade in form of a bi-directional scattering function (BSDF) matrix. BSDF matrices attribute the corresponding transmittance and reflectance values (front and back) to 145 solid angles, each of which represents a defined set of solar incidence angles. For materials with different reflection coefficients in the visible and the solar spectrum, *genbsdf* was run for both ranges separately. The BSDF matrices of shd 9 (fabric mesh) and shd 10 (metal mesh) were measured at the LBNL Solar Optical Properties Lab [11].

The resulting BSDF matrices were then imported into Window 7 [12] as new entries in the shading layer database. In the Window 7 glazing library the shading layers were added at the external side of the base glazing system described in Section 2.1.1 (see Table 2a). The resulting values for U-value, SHGC and Tvis under normal incidence can be found in Table 1.

2.1.4. Scalability

The annual energy results for the modeled shading systems can be transferred approximately to larger sized slat shading systems with the same geometry. In most exterior shading systems conductive heat transfer through the shade itself is negligible for the overall heat balance. The calculated convective heat transfer through the exterior shade is based on opening factors according to ISO 15099 in the simulation. The convective heat transfer between exterior shade and glazing system is treated separately and depends on the distance between the two. For high wind speeds and extreme conditions, computational fluid dynamics should be used for the assessment of convection through the shade and within the gap instead of the simplified approach used in this analysis. The long-wave emittance of the shading system, the visible and solar transmittance are fully scalable; i.e., the values remain the same if the geometrical relation stays the same but the dimensions are different.

2.2. Building energy simulation

2.2.1. Description of the commercial office building prototype

EnergyPlus building energy simulations [13] were used to evaluate the performance of the exterior shading systems in a prototypical large office building. Building prototypes are often abstract, synthetic buildings, not real buildings, that have been developed for the purpose of being representative of a population of buildings of a given type; e.g., office, hospital, etc.. Data are collected on real buildings and these data are used to formulate a statistical representation of building construction, systems, and operations. The US Department of Energy (DOE) has invested in the development of such prototypes over the past few decades and has made the prototypes publicly available for use by the building industry in order to standardize methods for evaluating technical measures and policies and to develop energy efficiency codes [14].

The original models are compliant with ASHRAE 90.1 and are available at [15]. The parameters of the building prototype used for this study have been modified to be code compliant with the California building code. Variations of this model are now available at [16] where users can also download the current Title 24 2013 certified code compliance software *CBECC-Com Nonresidential Compliance Software*, which is based on EnergyPlus version 8.0. (The presented results were calculated with EnergyPlus version 8.1 (released Oct 28, 2013) because of some additional features described below in Section 2.2.2 – 2.2.5.)

The large office prototype was defined as a 12-story, 48 m high building with a rectangular floor plate that is 73 m (north-south) by 49 m (east-west) (Appendix A). Perimeter zones were 4.57 m deep, with a 2.7 m ceiling height and a floor-to-floor height of 4 m. The perimeter zones were oriented in the four cardinal directions: due north, east, south, and west. The window-to-exterior-wall ratio was varied from 0 to 0.60 in order to quantify performance as a function of window area. No exterior obstructions were modeled.

The office prototype was defined with significant internal loads. Occupant density was 9.3 m^2 floor area per person. Occupancy was primarily between the hours of 9:00 to 17:00 on weekdays. Equipment loads were 8.1 W/m^2. Lighting loads were 7.5 W/m^2 at 100 % and reduced according to available daylight level for the case with daylighting controls (see also: Section 2.2.3. Scheduled Lighting Energy).

The building was conditioned using a variable air volume (VAV) system with a dry-bulb temperature controlled air-side economizer. An air-side economizer uses cool outdoor air on cold, but sunny days to meet the cooling load. The main air handler units serve the different building levels (ground, mid-floors, and top floor) while the air terminal units control the air flow from the main air handler unit to the individual zones through dampers. The minimum air flow of the air terminal units vary from 20 % to 30 % of the maximum air flow. Dampers are operated with a dual-maximum logic allowing the air flow in heating mode to be increased above the minimum air flow. The minimum outdoor air flow matches Title 24 requirements of 2.74 $m^3/(h\text{-}m^2_{floor})$ (0.15 cfm). The heating and cooling coils in the central plant and the reheat coils in the terminal units are auto-sized by EnergyPlus in every single run.

Site-to-source conversions of 3.3 for electricity and of 1.1 for gas were assumed. Natural gas is used in the model to heat the hot water boiler which serves the central heating coil as well as the reheat coils. Reheat coils are also operating when parts of the building are in cooling mode, therefore gas usage does not exclusively indicate if it is used for heating or cooling. In some of the cases, the reduction of cooling load significantly decreased the heating energy needed for reheat purposes due to the auto-sizing functionality of EnergyPlus.

In order to determine cooling and heating energy use by window orientation, cooling energy use associated with the centralized HVAC system was disaggregated to the north, east, south, and west perimeter zones based on airflow of the air terminal unit to the individual zones. The dead band for air temperature ranged from 21°C (setpoint temperature for heating) to 24°C (setpoint temperature for cooling) during occupied office hours.

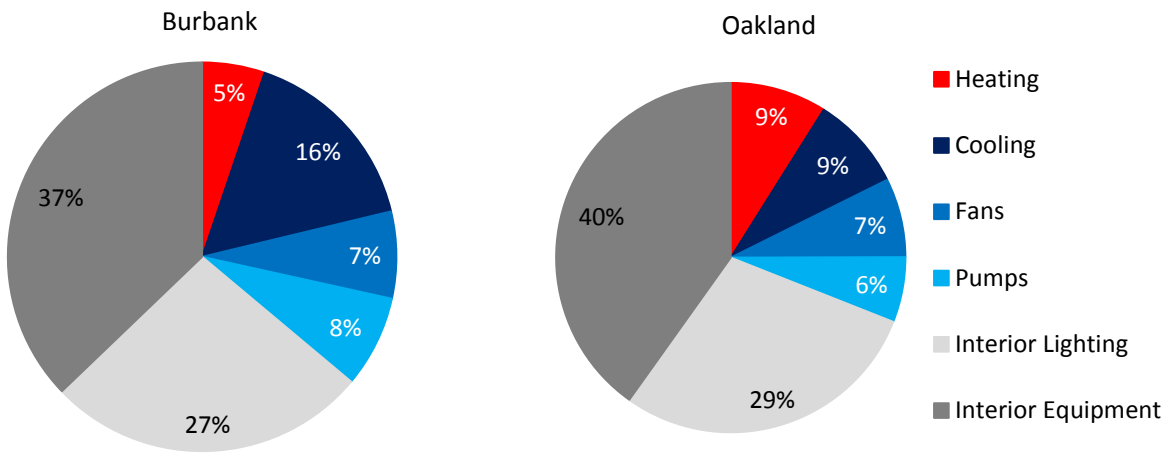

Fig. 2a. Site energy for the large office building prototype with the base glazing system and a window-to-wall-area ratio of 60 % (no daylighting controls).

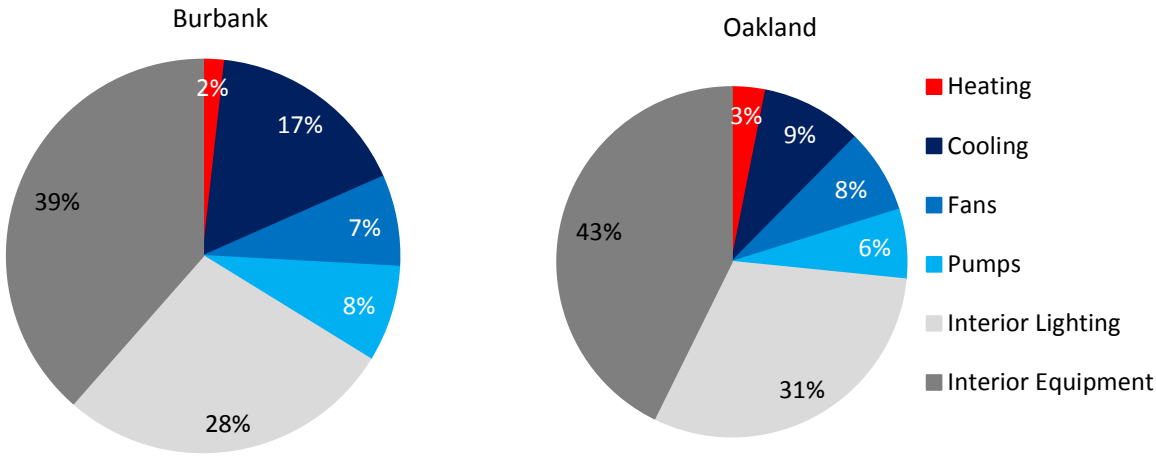

Fig. 2b: Source energy for the large office building prototype with the base glazing system and a window-to-wall-area ratio of 60 % (no daylighting controls). Electricity site-to-source conversion factor was 3.3. Natural gas site-to-source conversion factor was 1.1.

To give the reader a sense of the relative magnitude of energy required by the various end uses for the whole building, Figures 2a and 2b show the breakdown of site and source energy for the large office prototype with the base glazing and a window-to-wall ratio of 60 % (no shades, no daylighting controls) for Burbank and Oakland climate. For this building type, lighting and HVAC (cooling, heating, fans and pumps) account for more than the half of the energy end uses in commercial office buildings, and both are influenced by window and daylighting systems.

2.2.2. The method of "Scheduled Surface Gains"

The accurate calculation of window heat gains through complex fenestration systems and their distribution over the surfaces of interior walls and ceiling requires first a geometrical description of the CFS, and second it requires algorithms that consider the outgoing distribution of direct radiation (out of the façade into the room). With EnergyPlus V7.2 the "Klems-BSDF" [17, 18] method was added to the existing calculation method for window heat transfer, the "Winkelmann" [19] method. The newly implemented method is based on bi-directional scattering distribution function (BSDF) data and distributes transmitted radiation to the interior surfaces according to their outgoing angle. To facilitate the use of the "Klems-BSDF" method, the user can build the complex fenestration system in Window7 using the glazing and shading database and generate an output file that contains the objects of the input file in an EnergyPlus-compatible format.

With EnergyPlus V8.1, a method that was developed at LBNL over the past few years and had been used in an LBNL-internal EnergyPlus version, was implemented into the official release. It allows for an even more precise consideration of radiation heat transfer through the façade by facilitating user specific input. The method is referred to as "scheduled surface gains", and it allows the use of pre-calculated results for the solar energy that gets absorbed in the layers of the fenestration system and the amount of solar radiation that is incident on the interior surfaces in the room.

For this study, this solar energy was calculated using Radiance, a research-grade ray tracing software [20], as hourly values over the whole year and the results were provided as external files. EnergyPlus accesses the values for absorbed radiation in the CFS layers and on the surfaces of the perimeter zone through a

“schedule:file” object and the surfaces were referenced to these external files through newly introduced objects : “SurfaceProperty:SolarIncidentInside” and “ComplexFenestrationProperty:SolarAbsorbedLayers” In order to keep the computation time for calculating the absorbed solar radiation at bay, we used Radiance’s Three-Phase-Method [21, 22] for pre-calculation.

2.2.3. Scheduled Lighting Energy

Similarly to the scheduled surface gains, lighting energy use with daylighting controls in this study is based on Radiance simulation results. During occupied hours (using the occupancy schedule of the large office prototype with the 2009 calendar year) the illuminance was kept to a design level (500 lux). The Radiance output represents the percentage of maximum lighting power density (W/m^2) that is needed to maintain the target illuminance. The use of relative lighting power density allows for lower design illuminance values (e.g. 300 lux) and can account for more efficient light fixtures. The daylight saving calculation is based on the assumption that the maximum lighting power density (EnergyPlus input value, here: 7.5 W/m^2) is capable of providing the design illuminance. The relationship between light output and power use was assumed to be linear over the full range of dimming (i.e., 0-100% power, 0-100% light output).

2.2.4. Glare Control of Interior Shade with Energy Management System

Simulations of angular-selective systems [23] have shown the importance of daylight use for the total energy use of a building. According to the US Energy Information Administration, electric lighting energy accounts for 20 % of the site energy use in commercial buildings, and for 38 % of the electric energy [24]. In the simulation model used for our studies angular-selective systems with higher transmission of visible light tend to lead to lower whole building energy consumption even if their cooling load is elevated. However, without consideration of glare the simulation results lack validity because systems with high visible transmittance or systems with a significant portion of direct radiation coming into the space may produce glare which will cause the occupants to lower the interior shade, hence reduce interior daylight levels.

In this study, a glare-based control algorithm was used based on Radiance results for Discomfort Glare Probability (DGP) [25] and Discomfort Glare Index (DGI) [26] to control the deployment of the interior shade. The Radiance glare calculations are run prior to the actual simulation and a scheduled control algorithm based on the hourly results for DGP and DGI is used for the actuation of the interior shade.

The simulation model represents a large office building with open space office area in the perimeter zone. Nine viewpoints (i.e. work place positions) were used to evaluate the occurrence of glare and the degree of discomfort that it produces (see Fig. 3). As numerical limit when an interior shade has to be deployed because of glare, values of DGP $\geq$ 0.38 or DGI $\geq$ 24 for any of the viewpoints were chosen. The model for glare evaluation did not consider electric lighting in the space. The work-flow within the EnergyPlus simulation can be seen in Fig. 4. The user defined control algorithm assumed that the roller shade was lowered to cover the full height of the window at the first occurrence of discomfort glare and that it stayed there for the remainder of the day.

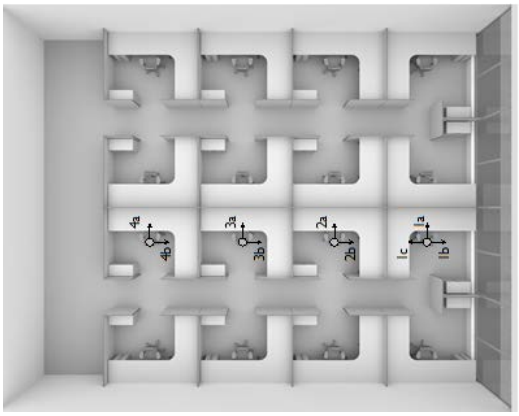

Fig. 3: Viewpoints of building model for glare evalution

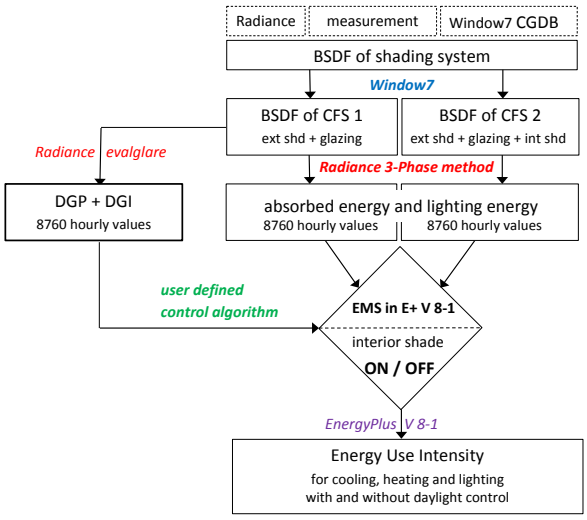

Fig. 4: Workflow in EnergyPlus

The Energy Management System (EMS) in EnergyPlus allows simulating an automated shading system based on any user defined control algorithm or schedule. With EnergyPlus V8-1 the possibility of using two shading layers (here: exterior and interior) and controlling them independently was implemented. Most building simulation programs do not allow for modeling two shading systems because of the interference of the scattering effect of shades or blinds. By adding two non-specular, scattering shading layer the problem shifts from a one-dimensional heat balance equation to a complex geometric calculation.

For the glare controlled simulation of exterior and interior shades, the “scheduled surface gains” method allowed us to use the ray-tracing approach of Radiance and is therefore best suited to describe the optical properties of a façade system with multiple shading layers.

3. Fixed exterior slat shading systems without interior shade

3.1. Influence of slat angle and cut-off angle on energy use intensity

In order to assess the impact of slat angle and cut-off angle for an exterior blind system with flat slats and a moderate reflectance (Rvis = Rsol = 0.5), the geometry of the commercially available product shd 2 was modified (see Table 3). The cut-off angle is defined as the highest profile angle at which direct radiation is transmitted into the space.

	shd 1	shd 2	shd 3	shd 4	shd 5
Slat angle (degree)	0	30	60	30	60
Cut-off angle (degree)	45	30	15	0	0
Ratio: slat width to spacing	1:1	1:1	1:1	1:0.5	1:0.86

Table 3: Variations of micro slat shading geometry

This section presents annual energy use intensity (EUI) in kWh/m^{2}a of a 4.5 m deep perimeter zone. A different trend for site vs. source energy can be related to the trade-off between admitted solar radiation, cooling and heating and the varying site-to-source conversion factors for electricity and natural gas.

The dark blue bars in the following Fig. 5 – 6 and Fig. 9 – 10 represent energy use that is not directly related to the window. It is based on simulation runs without any transparent area in the building envelope (window-to-wall ratio (WWR) = 0). The light grey bar is the energy use related to the window due to solar radiation and daylight, and the sum of dark blue and light grey is the total energy use as energy use intensity in kWh/m^{2}a.

3.1.1. Without daylighting controls

Fig. 5 shows site and source energy for Burbank and Fig. 6 shows site and source energy for Oakland for a relatively large window-to-wall ratio of 60 % (WWR 60) without daylighting control.

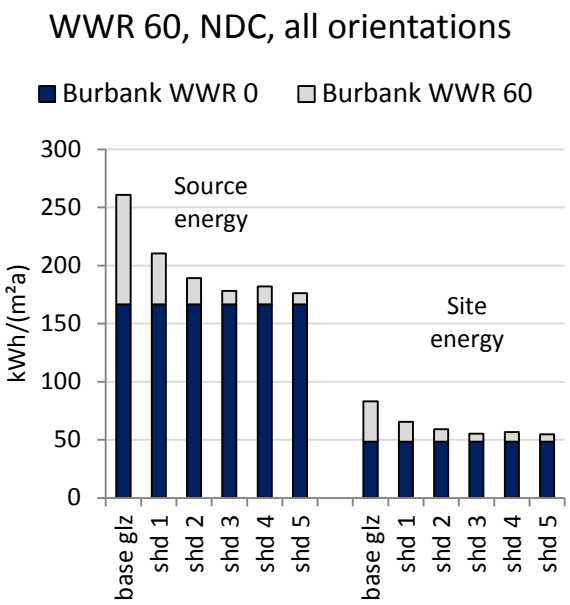

Figure 5: Source and site energy (HVAC and lighting) for a WWR of 60 % in Burbank without daylighting controls

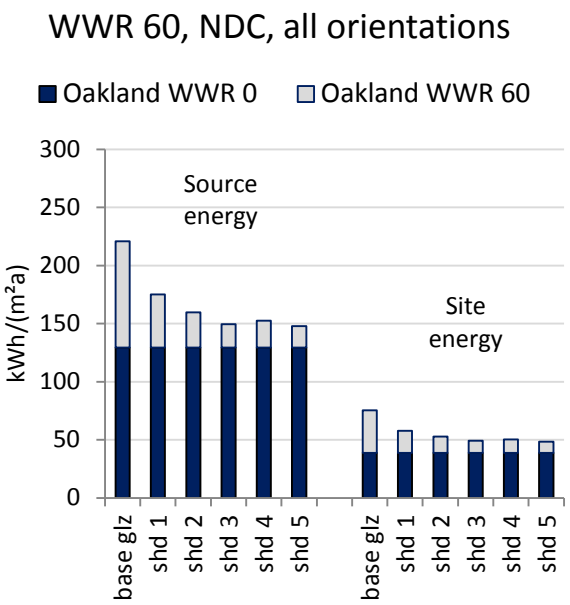

Figure 6: Source and site energy (HVAC and lighting) for a WWR of 60 % in Oakland without daylighting controls

In both climates, Burbank and Chicago, exterior shades reduce EUI significantly. Shd 5 as best performing shade for the case without daylighting controls reduces total source energy use by 85 kWh/m²a (32 %) in Burbank and by 73.2 kWh/m²a (33 %) in Oakland. This is a reduction of 90 % of the window related source energy for Burbank, and of 80 % in Oakland.

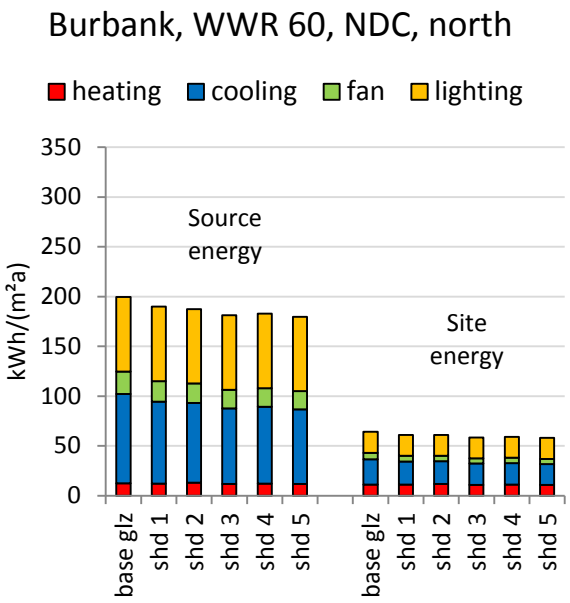

Figure 7a: Source and site energy of a north oriented perimeter zone for heating, cooling, fan, and lighting for a WWR of 60 % in Burbank without daylighting controls

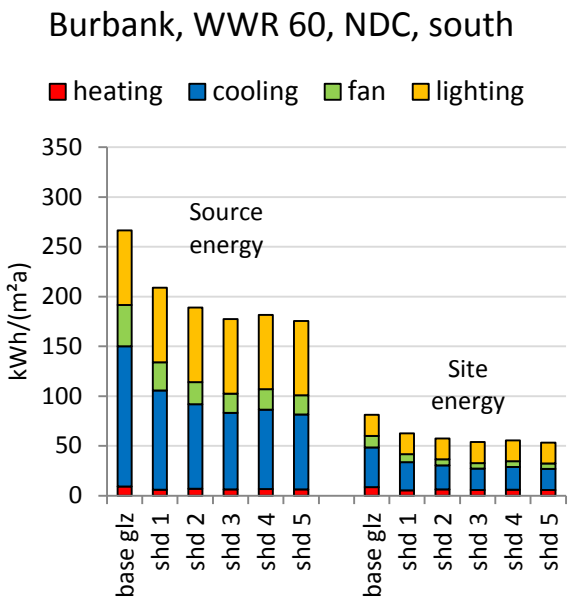

Figure 7b: Source and site energy of a south oriented perimeter zone for heating, cooling, fan, and lighting for a WWR of 60 % in Burbank without daylighting controls

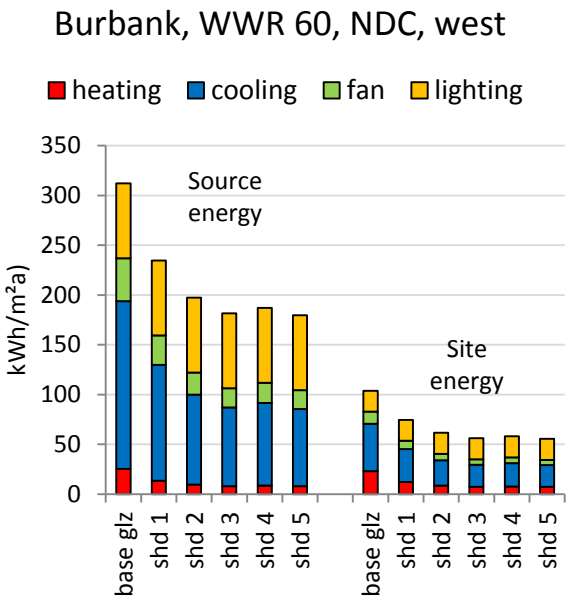

Figure 7c: Source and site energy of a west oriented perimeter zone for heating, cooling, fan, and lighting for a WWR of 60 % in Burbank without daylighting controls

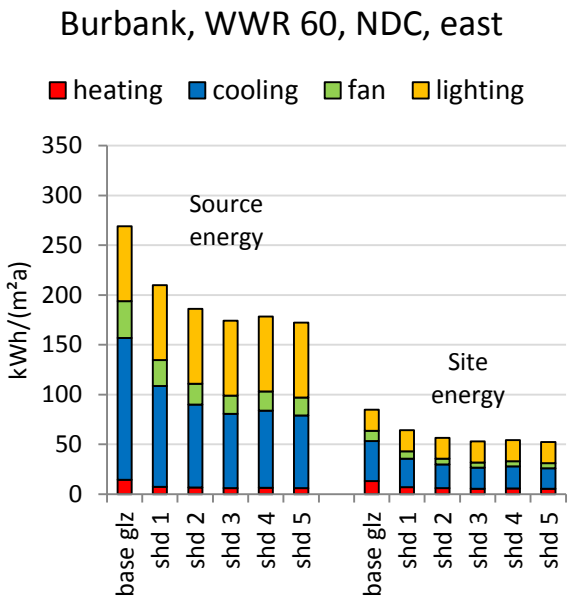

Figure 7d: Source and site energy of an east oriented perimeter zone for heating, cooling, fan, and lighting for a WWR of 60 % in Burbank without daylighting controls

Fig. 7 – 8 (Fig 11 – 12) split site and source energy for Burbank and Oakland into heating, cooling, fan and lighting for the four orientations. The energy quantities are disaggregated to the different orientations according to the air flow of the VAV terminal units into the single zones. In this section results are shown only for large windows with a WWR 60.

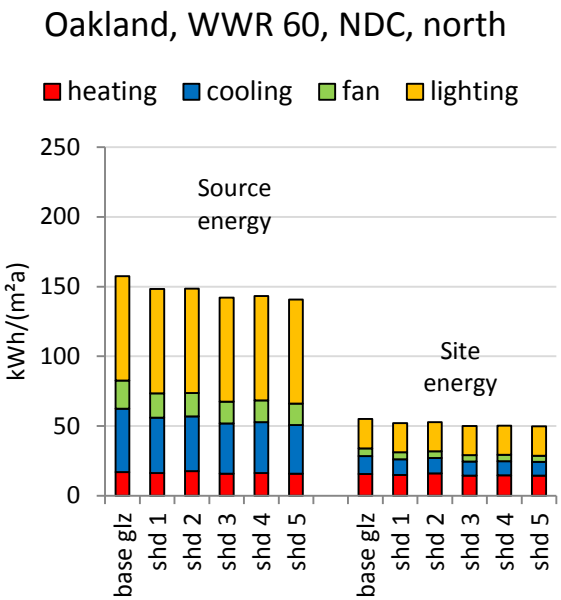

Figure 8a: Source and site energy of a north oriented perimeter zone for heating, cooling, fan, and lighting for a WWR of 60 % in Oakland without daylighting controls

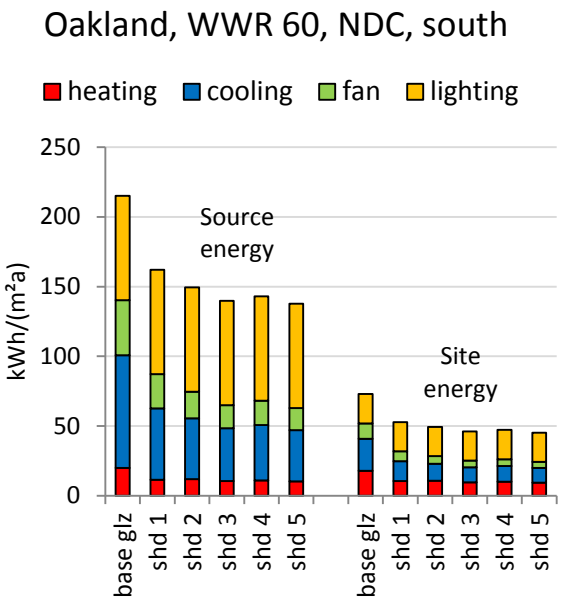

Figure 8b: Source and site energy of a south oriented perimeter zone for heating, cooling, fan, and lighting for a WWR of 60 % in Oakland without daylighting control

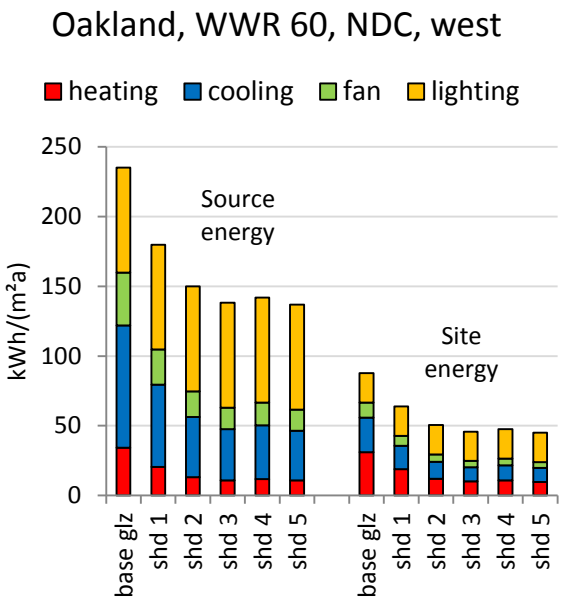

Figure 8c: Source and site energy of a west oriented perimeter zone for heating, cooling, fan, and lighting for a WWR of 60 % in Oakland without daylighting controls

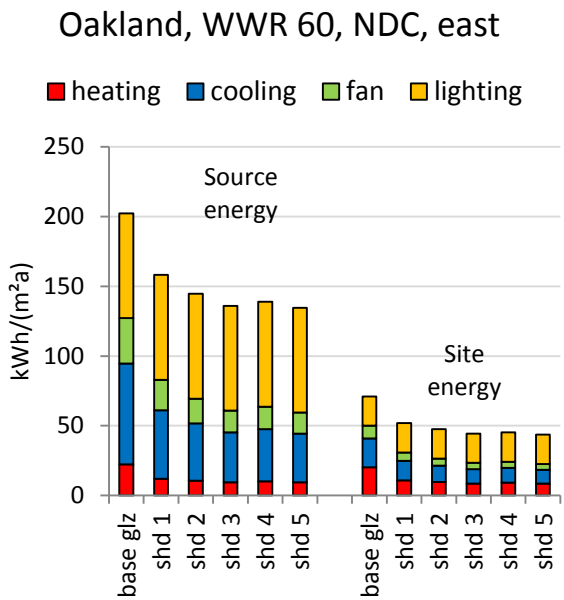

Figure 8d: Source and site energy of an east oriented perimeter zone for heating, cooling, fan, and lighting for a WWR of 60 % in Oakland without daylighting controls

In Burbank, the energy use intensity for heating is small compared to cooling, fan, and lighting. Site and source energy follow therefore the same trend. Cooling is the predominant energy type required for the case without

exterior shade, followed by lighting energy which is constant as there is no daylighting control assumed in this section. Fan energy increases proportionally with cooling energy.

In Burbank, the highest overall EUI without exterior shade can be found on the west facade, while south and east façade show similar values. The best performing slat geometry is shd 5 for all orientations, and the highest absolute and relative reduction of total source energy can be achieved on the west façade where the source EUI is reduced by 132.4 kWh/m²a (42 %). For east and south orientation reductions are 91.5 - 96.8 kWh/m²a (34 - 36 %), and for north orientation a reduction of 20.4 kWh/m²a (10 %) was obtained.

In Oakland, if no daylighting controls are installed, lighting energy represents the biggest portion of total energy use intensity for the cases with exterior shade. Site heating energy, if averaged over all orientations, is of the same order of magnitude as site cooling, and greater than site fan energy. When looking at source energy, lighting energy dominates EUI for north, south and east orientation, followed by cooling, fan and heating energy. Only for south and west orientation without exterior shade, cooling energy is slightly higher than lighting energy.

Like in Burbank, the best performing slat geometry is shd 5 for all orientations, and the absolute and relative reduction of total source energy on the west is 98 kWh/m²a (42 %). For east and south orientation reductions of 65.6 - 77.5 kWh/m²a (33-36 %), and for north orientation of 16.1 kWh/m²a (11 %) were obtained.

3.1.2. With daylighting controls

Fig. 9 and 10 show site and source energy for Burbank and Oakland for a window-to-wall ratio of 60 % (WWR 60) and with daylighting controls. The light blue bars in the graphs represent cases where total source energy is below the no-window related EUI. The white contours on top of the light blue bars represent the savings compared to a purely opaque wall. I.e. for a window-to-wall ratio of 60 % all exterior slat shading systems reduce EUI compared to the not-shaded case in Burbank and in Oakland when averaged over all orientations.

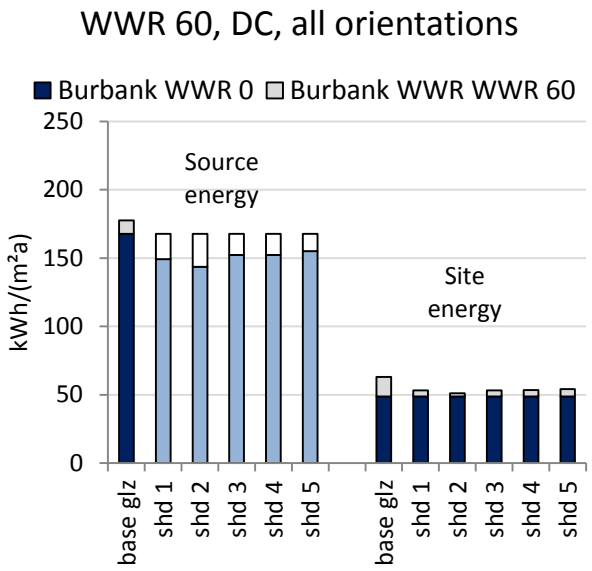

Figure 9: Source and site energy (HVAC and lighting) for a WWR of 60 % in Burbank with daylighting controls

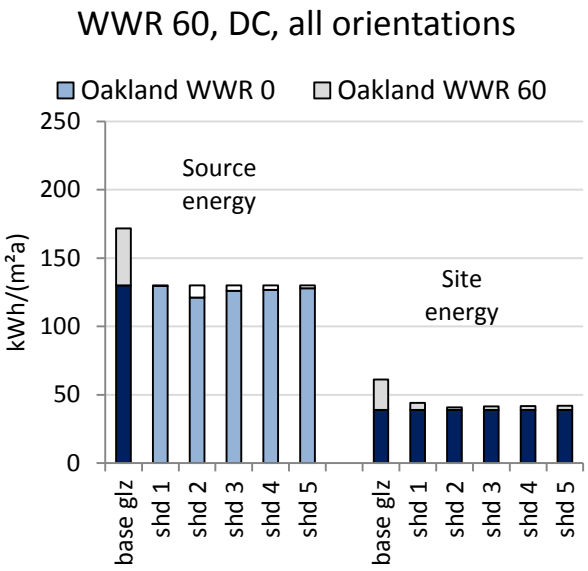

Figure 10: Source and site energy (HVAC and lighting) for a WWR of 60 % in Oakland with daylighting controls

With daylighting control, shd 2 is the best performing shade in terms of source energy and reduces total source energy use by 34.4 kWh/m²a (19 %) in Burbank and by 50.6 kWh/m²a (30 %) in Oakland. This is a total

elimination of the window related source energy for both, Burbank and Oakland. The relative savings are less for the case with daylighting controls, because daylighting controls work best for highly transmissive facades.

The interaction of daylighting controls and exterior shades strongly depend on the orientation. While all exterior shades were beneficial to reduce source and site energy on any orientation when there were no daylighting controls assumed, the use of photosensors to dim artificial lighting when daylight is available changes this trend significantly. With daylighting controls, the only exterior shade that does not raise EUI in a north facing office is shd 1with its relatively high cut-off angle of 45 ° (see Fig. 11a and 12a).

In Burbank, when looking at south, east and west façades, the trade-offs between cooling and lighting become obvious: the more blocking shades (shd 3 – 5) reduce cooling energy but require more lighting energy. With shd 1, the lowest lighting energy of all exterior shade systems can be obtained, although the higher EUI for cooling energy and related increased energy for reheat offsets these savings for all but the north orientation.

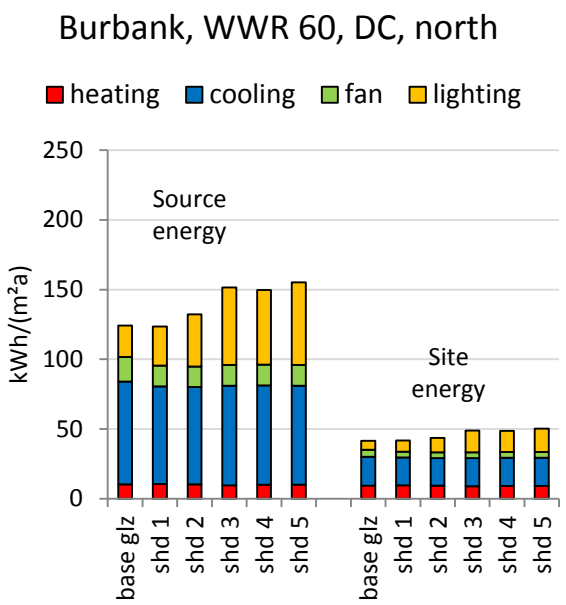

Figure 11a: Source and site energy of a north oriented perimeter zone for heating, cooling, fan, and lighting for a WWR of 60 % in Burbank with daylighting controls

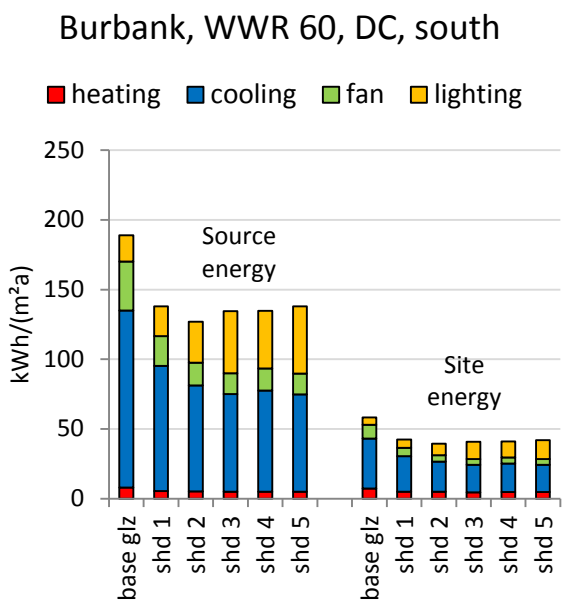

Figure 11b: Source and site energy of a south oriented perimeter zone for heating, cooling, fan, and lighting for a WWR of 60 % in Burbank with daylighting controls

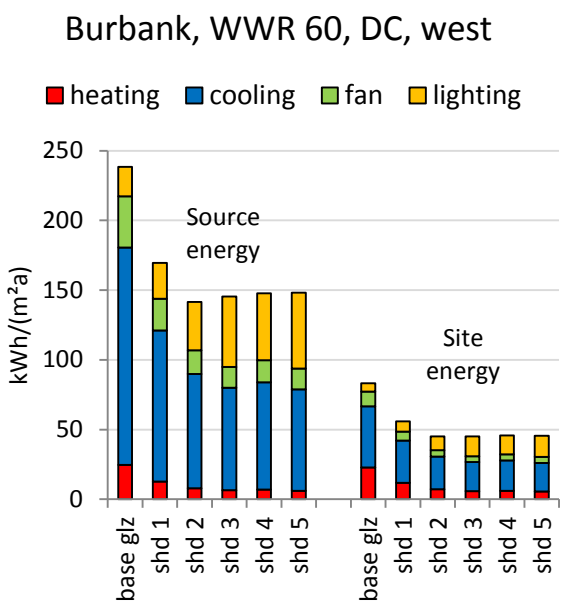

Figure 11c: Source and site energy of a west oriented perimeter zone for heating, cooling, fan, and lighting for a WWR of 60 % in Burbank with daylighting controls

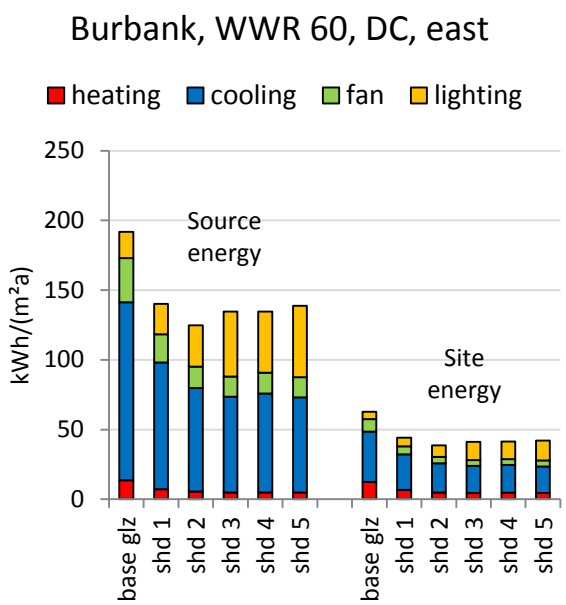

Figure 11d: Source and site energy of an east oriented perimeter zone for heating, cooling, fan, and lighting for a WWR of 60 % in Burbank with daylighting control

In Oakland, where cooling energy is not as predominant as in Burbank, shd 1 shows also good performance for south and east orientation mainly due to the reduction of lighting energy because of the higher cut-off angle that allows for more daylight. With shd 2, the minimum EUI can be obtained for both Burbank and Oakland climates on east, south and west orientations.

Maximum reductions for Burbank are 66.7 kWh/m²a (35 %) for east, 62.4 kWh/m²a (33 %) for south, and 96.8 kWh/m²a (41 %) for west orientation. In Oakland maximum reductions are 44.1 kWh/m²a (31 %) for east, 52.7 kWh/m²a (35 %) for south, and 71 kWh/m²a (41 %) for west orientation.

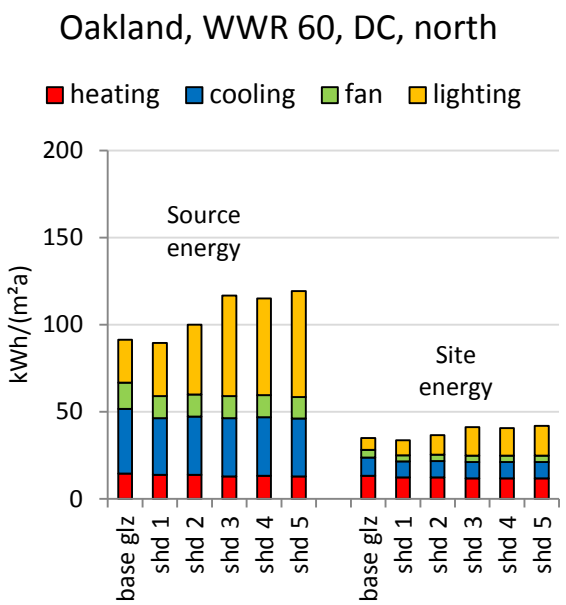

Figure 12a: Source and site energy of a north oriented perimeter zone for heating, cooling, fan, and lighting for a WWR of 60 % in Oakland with daylighting controls

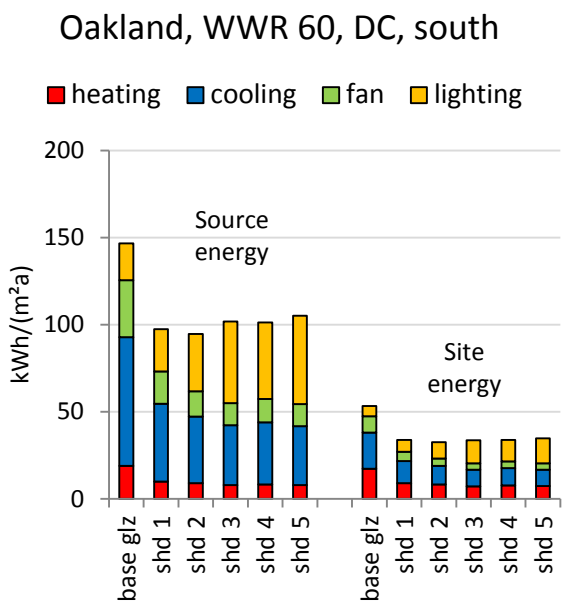

Figure 12b: Source and site energy of a south oriented perimeter zone for heating, cooling, fan, and lighting for a WWR of 60 % in Oakland with daylighting controls

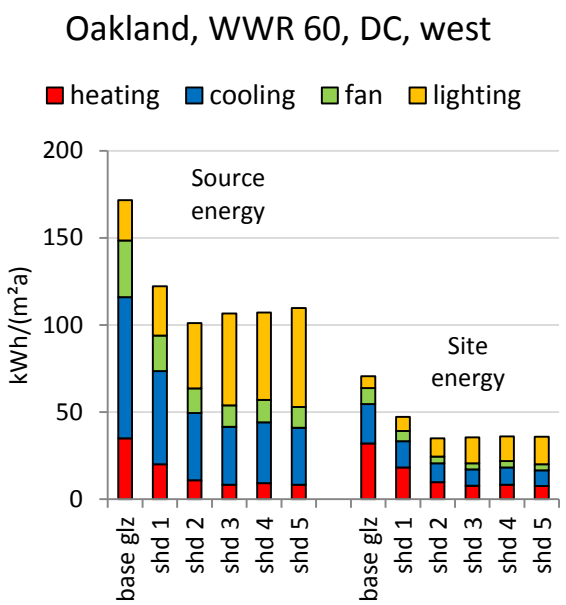

Figure 12c: Source and site energy of a west oriented perimeter zone for heating, cooling, fan, and lighting for a WWR of 60 % in Oakland with daylighting controls

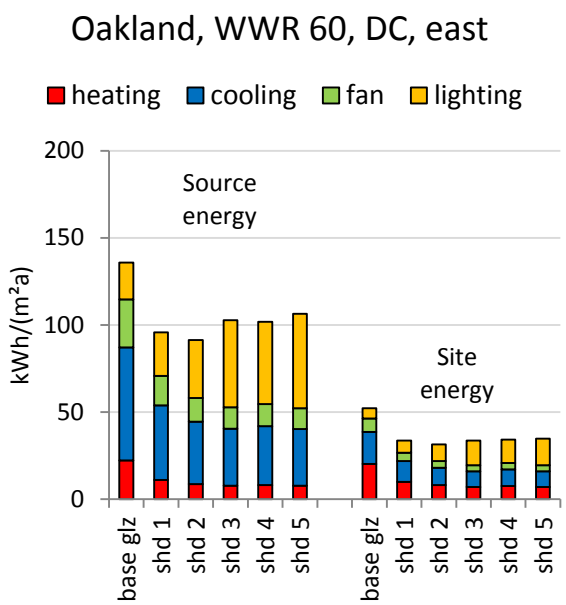

Figure 12d: Source and site energy of an east oriented perimeter zone for heating, cooling, fan, and lighting for a WWR of 60 % in Oakland with daylighting controls

3.2. Influence of surface properties on energy use intensity

The variations of shd 7 are based on a commercially available, retractable shade. It is available in a variety of colors which possess different optical properties. In order to assess the influence of the surface property on energy performance, three different surfaces were chosen: “Miro” (shd 7a), a highly reflective slat, “Gray” (shd 7b) a low reflective slat, and “Selective” (shd 7c) a slat with higher reflectance in the visible range than in the solar spectrum (for material properties see Table 2a-c, for geometry see Appendix B). Fig. 13 shows the EUI for a south façade in Burbank with and without daylighting controls, and Fig. 14 shows the EUI for a west façade. Fig. 15 and 16 show the EUI for a south façade and west façade respectively in Oakland, with and without daylighting controls.

The highly reflective surface leads to a slight increase in cooling energy for the case without daylighting controls (south and west) compared to the shades with lower reflectance (shd 7b and 7c) due to the higher amount of solar radiation that is reflected into the space.

In the case of daylighting controls, the visible part of the additional radiation helps saving electric lighting energy and the reduction of lighting energy (i.e. reduction of cooling load) equalizes the cooling energy which is approximately constant amongst the three different surface properties. The increased daylight availability of shd 7a leads to the lowest total EUI values on both, the south and the west façade, for both climates, Burbank and Oakland.

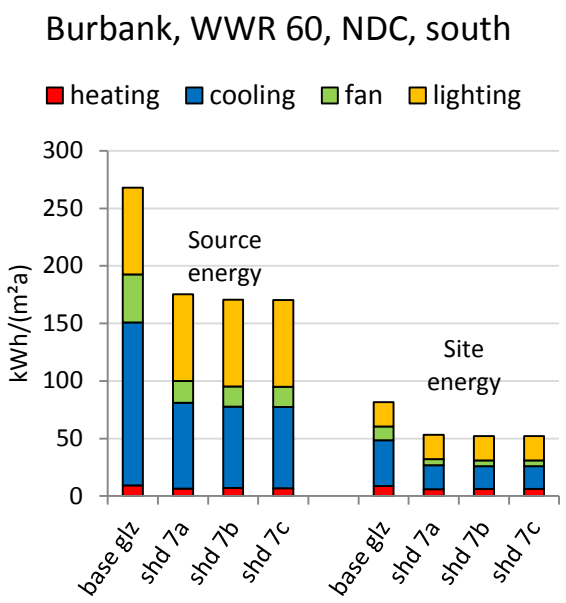

Figure 13a: Source and site energy of a south oriented perimeter zone for heating, cooling, fan, and lighting for a WWR of 60 % in Burbank without daylighting controls for shades with different optical properties

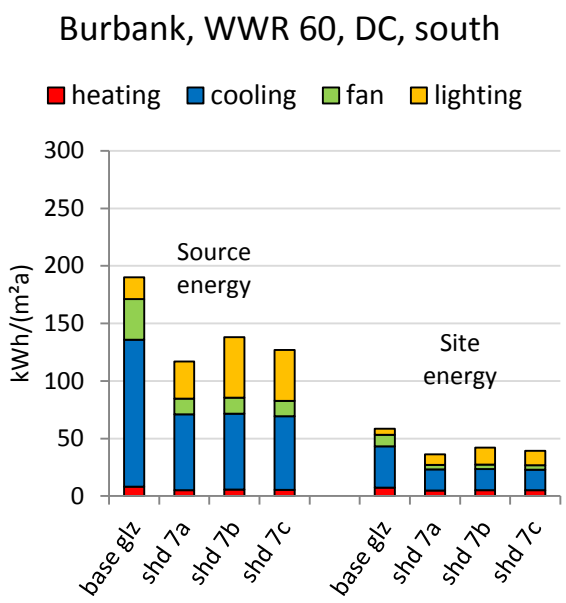

Figure 13b: Source and site energy of a south oriented perimeter zone for heating, cooling, fan, and lighting for a WWR of 60 % in Burbank with daylighting controls with different optical properties

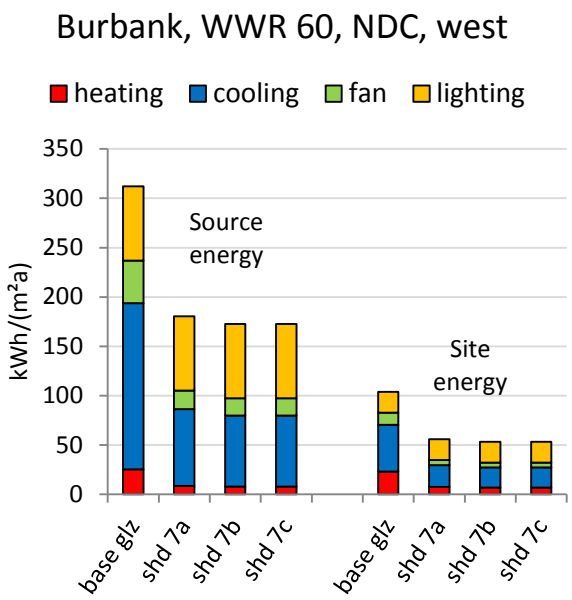

Figure 14a: Source and site energy of a west oriented perimeter zone for heating, cooling, fan, and lighting for a WWR of 60 % in Burbank without daylighting controls for shades with different optical properties

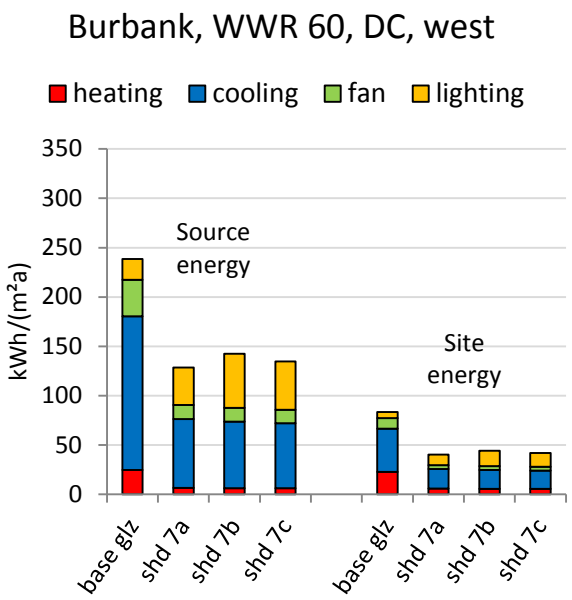

Figure 14b: Source and site energy of a west oriented perimeter zone for heating, cooling, fan, and lighting for a WWR of 60 % in Burbank with daylighting controls for shades with different optical properties

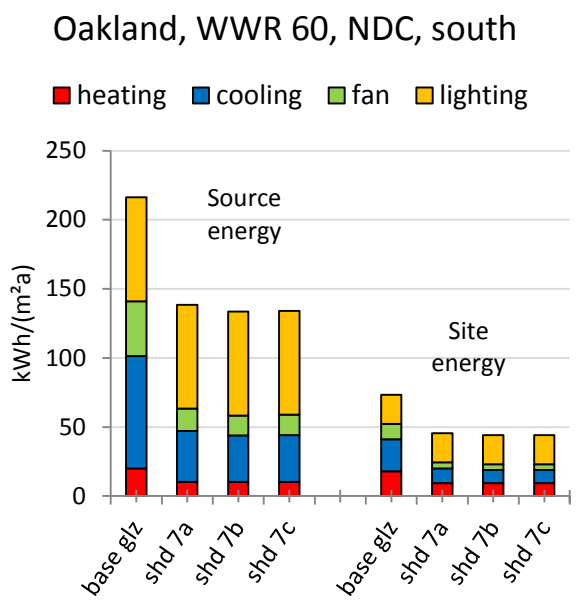

Figure 15a: Source and site energy of a south oriented perimeter zone for heating, cooling, fan, and lighting for a WWR of 60 % in Oakland without daylighting controls for shades with different optical properties

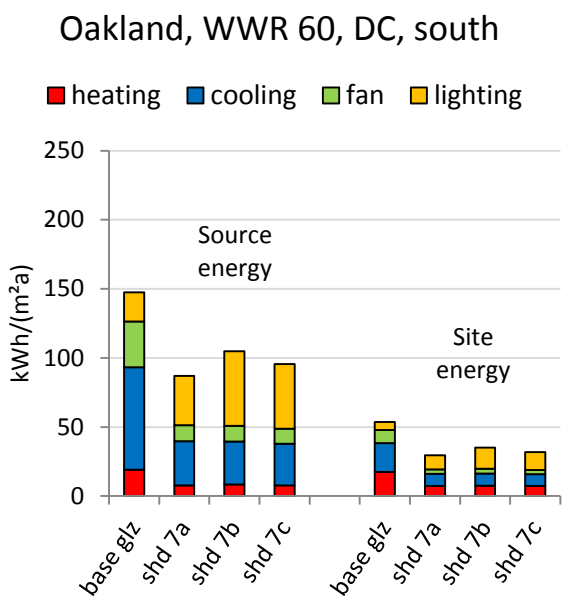

Figure 15b: Source and site energy of a south oriented perimeter zone for heating, cooling, fan, and lighting for a WWR of 60 % in Oakland with daylighting controls for shades with different optical properties

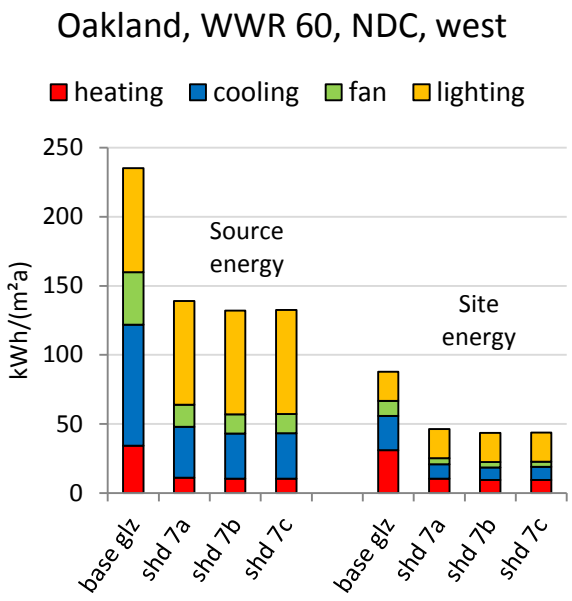

Figure 16a: Source and site energy of a west oriented perimeter zone for heating, cooling, fan, and lighting for a WWR of 60 % in Oakland without daylighting controls for shades with different optical properties

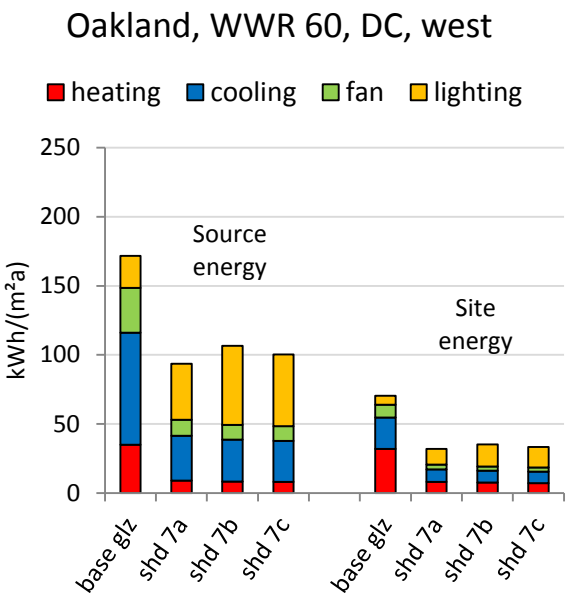

Figure 16b: Source and site energy of a west oriented perimeter zone for heating, cooling, fan, and lighting for a WWR of 60 % in Oakland with daylighting controls with different optical properties

4. Influence of glare on energy use intensity

While the previous Section 3.2 showed a benefit of highly reflective surfaces on exterior blinds when using daylighting controls, it did not consider the possibility of discomfort glare.

Not only direct radiation can lead to discomfort glare but light that is reflected from the shade into the room may also contribute to a situation where visual comfort at a workstation cannot be maintained without the use of an interior shade. The probability of glare conditions in the perimeter zone of an office with exterior shades therefore depends on a variety of parameters, e.g. the cut-off-angle for direct radiation, the geometry of the shade and the reflectance and transmittance of its material.

East and west orientations experience the most frequent glare conditions because of the low solar incidence angle. Table 4 shows that the number of hours with an occurrence of discomfort glare is similar for east and west facades, while the number of hours with the interior shade down is significantly higher for east orientation than for west orientation due to the assumed behavior (see Section 2.2.4).

The following Fig. 17 – 20 show the energy use intensity in Burbank and Oakland for an east and a west oriented perimeter zone (WWR 60) with and without daylighting controls. The graphs show the cases without exterior shade for reference and for the five exterior shades with the most frequent occurrence of discomfort glare (highlighted in Table 4).

	Number of hours with discomfort glare for one of the viewpoints						Number of hours with interior shade deployed					
	Burbank			Oakland			Burbank			Oakland		
	East	South	West	East	South	West	East	South	West	East	South	West
no shade	3569	3575	3640	3338	3324	3428	6052	5886	5778	5816	5681	5536
shd 1	3623	3300	3648	3375	3088	3436	6051	5863	5778	5813	5680	5541
shd 2	1296	1385	1346	1072	1312	1264	5831	3240	3742	5176	3390	3519
shd 3	212	0	121	127	0	89	3677	0	966	2190	0	606
shd 4	0	0	0	0	0	0	0	0	0	0	0	0
shd 5	0	0	0	0	0	0	0	0	0	0	0	0
shd 6	257	0	190	177	0	170	4067	0	1390	2672	0	1092
shd 7a	862	660	970	706	597	802	5232	1907	3171	4025	2041	2716
shd 7b	432	14	472	349	14	378	4805	197	2658	3444	197	2147
shd 7c	469	9	409	385	21	336	4783	90	2401	3553	172	1952
shd 8[6]	1145	1089	1199	954	1021	1071	5771	2653	3549	4895	2680	3216
shd 9[5]	1036	922	1097	878	884	977	5533	2129	3447	4686	2268	3108
shd 10[5]	1387	1587	1490	1212	1547	1367	5842	3654	3870	5244	3804	3640

Table 4: Frequency of glare and frequency of interior shade deployment, window-to-wall ratio 60 %, highlighted are the systems with the highest number of discomfort glare and which are shown in Fig.17 – 20

4.1. Without daylighting control

Fig. 17 - 18 show similar trends for both climates and both orientations. When comparing the case without exterior shade and no interior shade (base glazing, no interior shade) to the glare controlled case (base glazing, interior shade deployed when discomfort glare occurs and stays down until the next morning) the reduction of total source energy through an interior shade is much less than the reduction one can achieve with any of the exterior shades. Even shd 1 as the exterior shade with the highest cut-off angle, reduces EUI by twice as much as an interior shade for glare control does.

When we compare the case without interior shade to the case where an interior shade is deployed for glare control, only the base glazing performs better with glare control due to the additional reduction of solar

[6] In addition to the slat shading systems (shd 1 and shd 2, shd 8 represents aluminum louvers (Rvis = Rsol = 0.7) at a slat angle of 45 deg and a cut-off angle of 30 deg. Shd 9 and shd 10 are perforated meshes for which the transmission values have been measured with a goniophotometer at LBNL [11].

radiation through the interior shade. The total source EUI of the cases with exterior shades actually increases when glare control is applied.

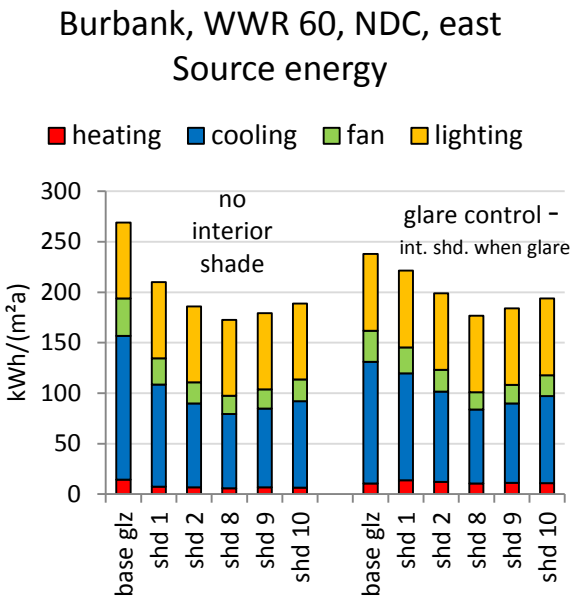

Figure 17a: Source and site energy of an east oriented perimeter zone for heating, cooling, fan, and lighting for a WWR of 60 % in Burbank without daylighting controls for the five shades with the highest glare occurrence

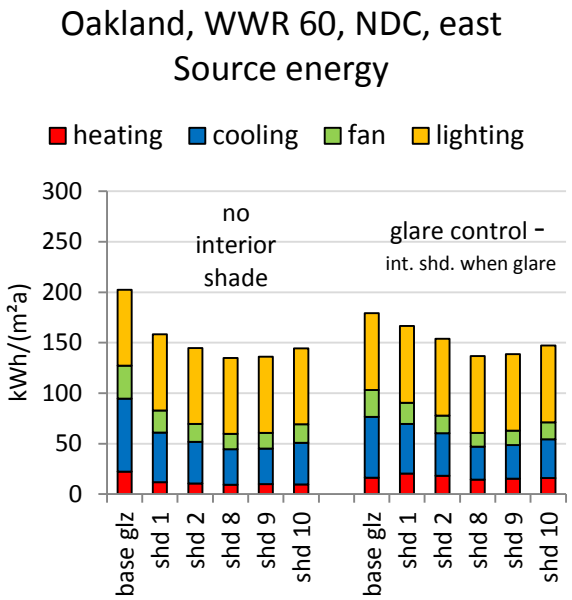

Figure 17b: Source and site energy of an east oriented perimeter zone for heating, cooling, fan, and lighting for a WWR of 60 % in Oakland without daylighting controls for the five shades with the highest glare occurrence

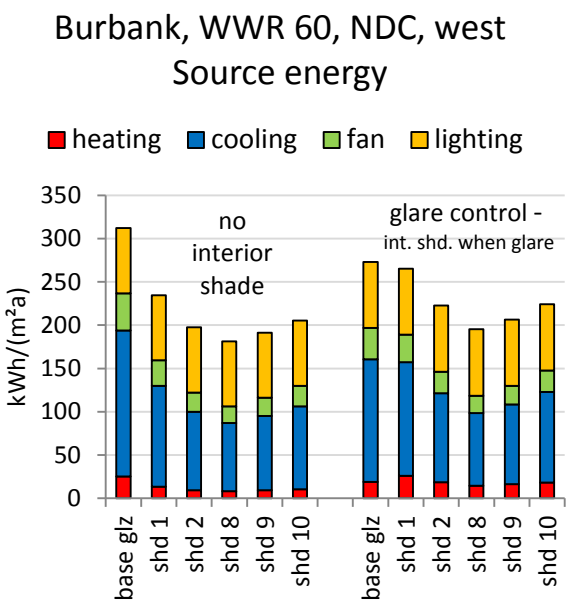

Figure 18a: Source and site energy of a west oriented perimeter zone for heating, cooling, fan, and lighting for a WWR of 60 % in Burbank without daylighting controls for the five shades with the highest glare occurrence

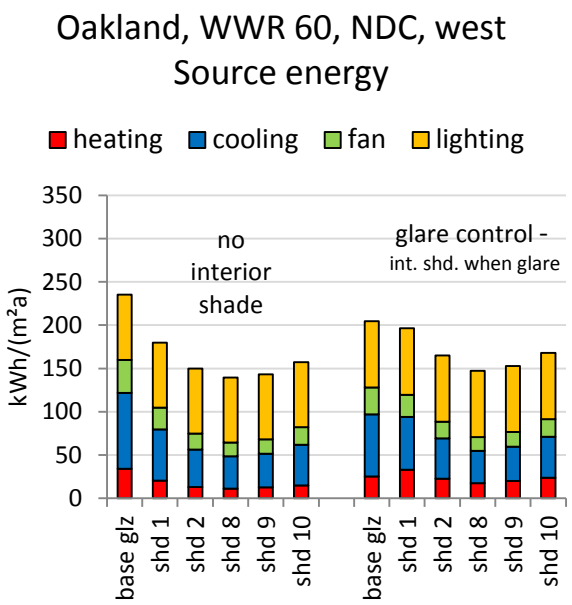

Figure 18b: Source and site energy of a west oriented perimeter zone for heating, cooling, fan, and lighting for a WWR of 60 % in Oakland without daylighting controls for the five shades with the highest glare occurrence

In both climates, Burbank and Oakland, the heating energy increases if an interior shade is deployed in addition to the exterior shade, while the cooling energy remains approximately the same. The only significant reduction of cooling energy is achieved for the case without exterior shade. Without daylighting control, the maximum

increase of total source EUI of the five exterior shading systems ranges from 6 – 7 % for west orientation and from 2 – 4 % for east orientation.

4.2. With daylighting control

While for the base glazing itself there was a benefit of glare control without daylighting control, with daylighting controls the total source EUI of the base glazing case as well as the EUI of all five exterior shade cases increases when glare control is applied. The increase in EUI is mainly due to increased lighting energy. For the base glazing without exterior shade, the increase in electric lighting due to lower daylight availability even offsets the reduction of cooling energy.

While without daylighting controls there was no major systematic difference between east and west orientation, a different trend can be seen when daylighting controls are used. On the east façade, source EUI increases drastically for all of the systems since on days where discomfort glare control is needed, the interior shade stays down for most of the day and blocks daylight for lighting and solar radiation for heating. On the west façade, the highest increase of source EUI occurs for shd 1. In Burbank, EUI for shd 2, 8, 9, and 10 are still strongly affected by the applied glare control due to an increase in lighting energy, while in Oakland lighting energy is less impacted for all but shd 1.

With daylighting control, the maximum increase of total source EUI of the five exterior shading systems ranges from 24 – 31 % for east orientation and from 26 – 29 % for west orientation.

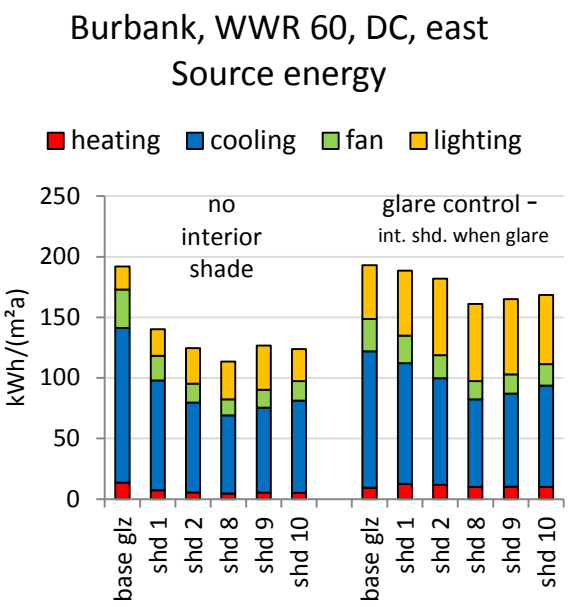

Figure 19a: Source and site energy of an east oriented perimeter zone for heating, cooling, fan, and lighting for a WWR of 60 % in Burbank without daylighting controls for the five shades with the highest glare occurrence

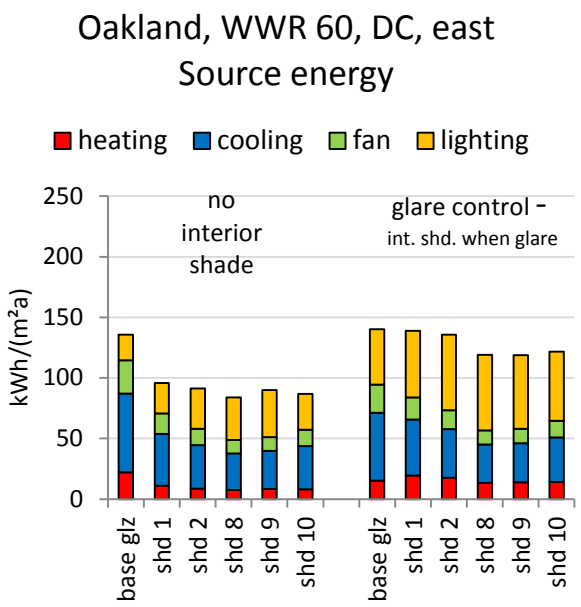

Figure 19b: Source and site energy of an east oriented perimeter zone for heating, cooling, fan, and lighting for a WWR of 60 % in Oakland with daylighting controls for the five shades with the highest glare occurrence

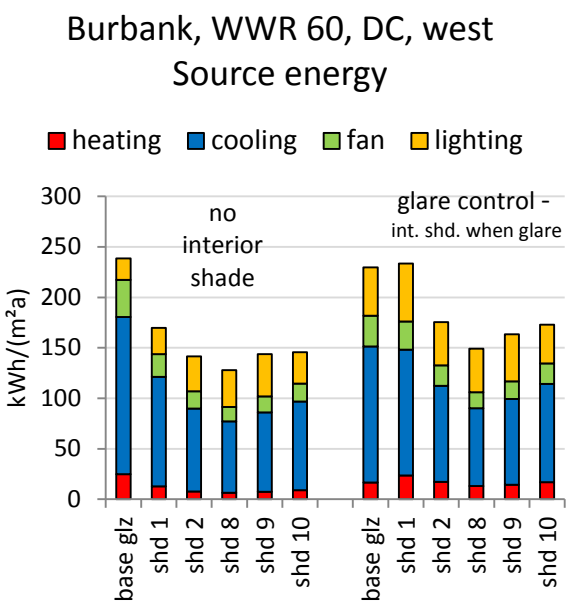

Figure 20a: Source and site energy of a west oriented perimeter zone for heating, cooling, fan, and lighting for a WWR of 60 % in Burbank with daylighting controls for the five shades with the highest glare occurrence

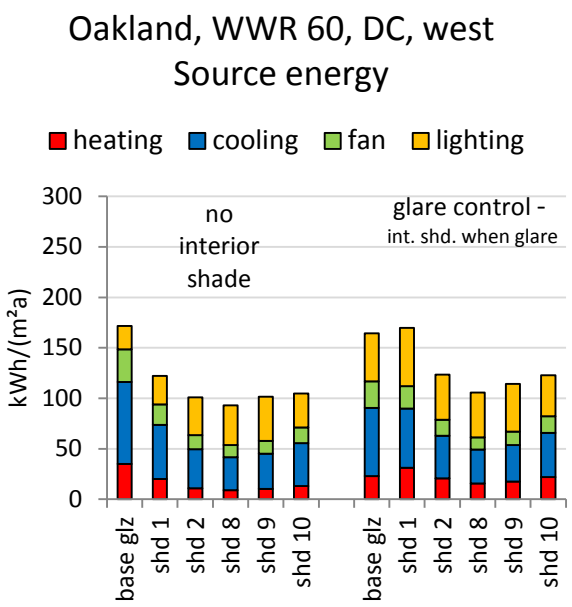

Figure 20b: Source and site energy of a west oriented perimeter zone for heating, cooling, fan, and lighting for a WWR of 60 % in Oakland with daylighting controls for the five shades with the highest glare occurrence

5. Energy use intensity depending on window-to-wall ratio with daylighting control and glare control

Section 4 has shown that the impact of glare control on the overall source energy use intensity is minor when no daylighting controls are installed. However, when electric lighting is dimmed according to daylight availability, the deployment of an interior shade to avoid discomfort glare reduces significantly the energy savings that can be achieved with exterior shades on facades with a WWR of 60 %.

To assess this impact further, this section contains results for all exterior shading systems with and without glare control for east and west orientation, and with daylighting controls installed. In the following figures, the source energy use intensity of a prototypical large office building with exterior shades is compared to a code compliant Title 24 (2013) building without exterior shades. EUI is shown for source energy over four different WWR. Intermediate WWRs are interpolated.

Code reference EUI:

The base glazing (see Table 1) without exterior shade and without interior shade is used as reference curve for code compliance. The dark gray area represents EUI values of 50 % of the code reference value or less. Title 24 requests a limitation of WWR to 40 % for the standard model. Here, the code EUI (and subsequently the 50 % code EUI) was capped at WWR 45 %. No glare control was assumed for the code reference case, so the reference line remains the same independent if glare control is applied for the exterior shades or not. The red numbers in the graphs show the percentage savings that the best performing shading system achieves for a given WWR (0, 15, 30, 45, 60 %).

5.1. East orientation

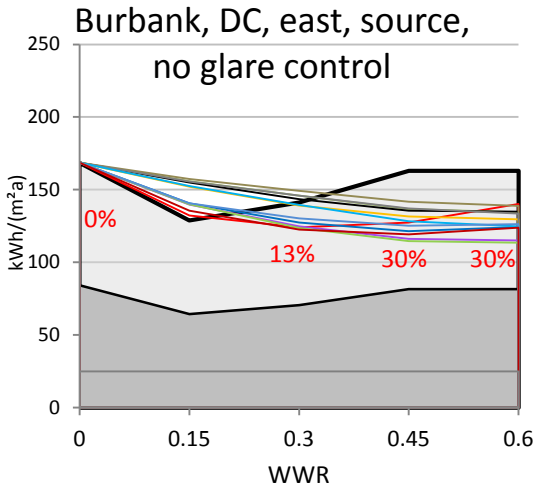

Figure 21a: Total source energy with daylighting control and without glare control in Burbank on an east facade.

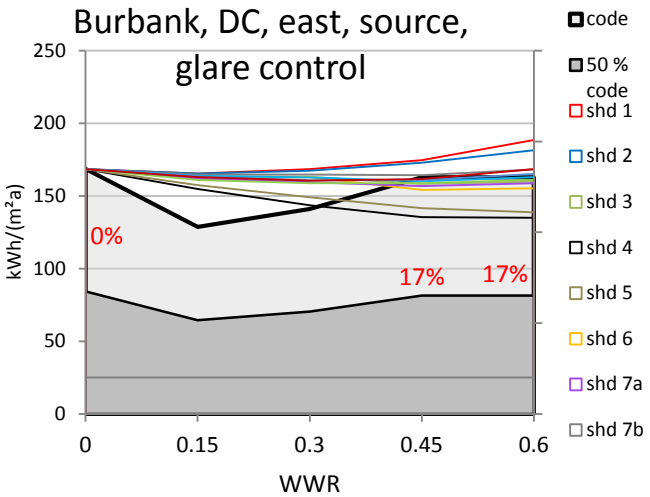

Figure 21b: Total source energy with daylighting control and with glare control in Burbank on an east facade.

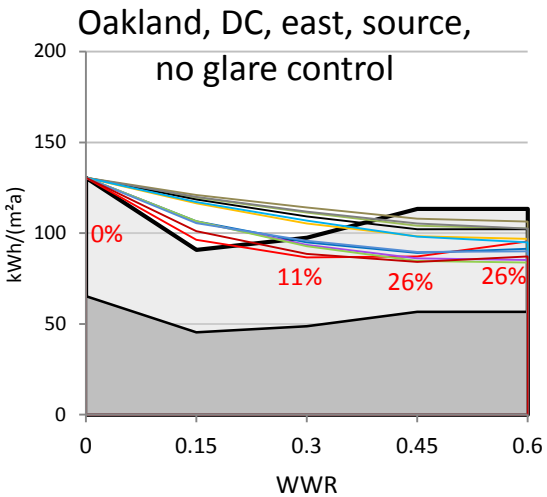

Figure 22a: Total source energy with daylighting control and without glare control in Oakland on an east facade.

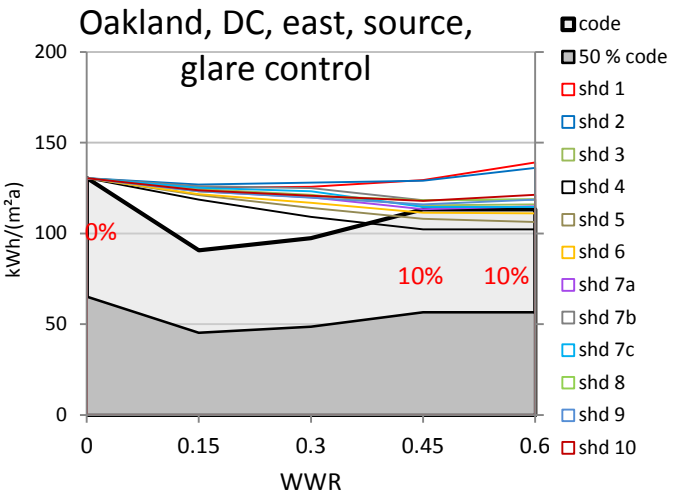

Figure 22b: Total source energy with daylighting control and with glare control in Oakland on an east facade.

Without glare control, the maximum savings that can be achieved on the east façade for WWRs ≥ 45 % are 30 % for Burbank and 26 % for Oakland. The energy savings for the more blocking shades (shd 3, shd 4, shd 5) are small for large windows while the most reflective shades (shd 7a, shd 8) show the lowest EUI. When using glare control in the simulation, this trend changes: now the most blocking shades without an occurrence of glare (shd 4 and shd 5) perform best. However, with glare control their energy saving potential is only 17 % for Burbank and 10 % for Oakland. Most other exterior shades show little benefit compared to the reference case.

For WWRs ≤ 30 % there are only few exterior shades that achieve EUIs below the code reference without glare control, and with glare control none of the exterior shades saves energy compared to code reference.

5.2. West orientation

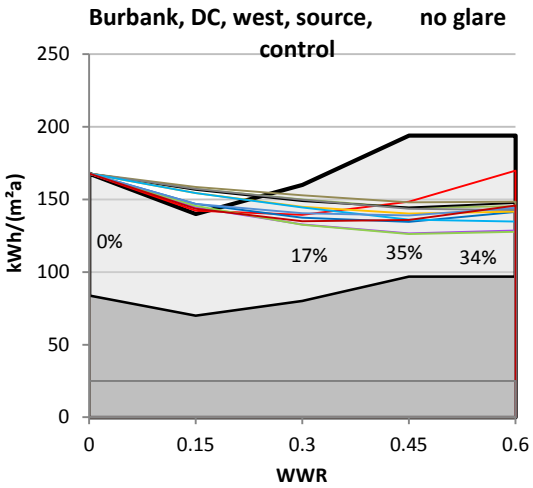

Figure 23a: Total source energy with daylighting control and without glare control in Burbank on a west facade.

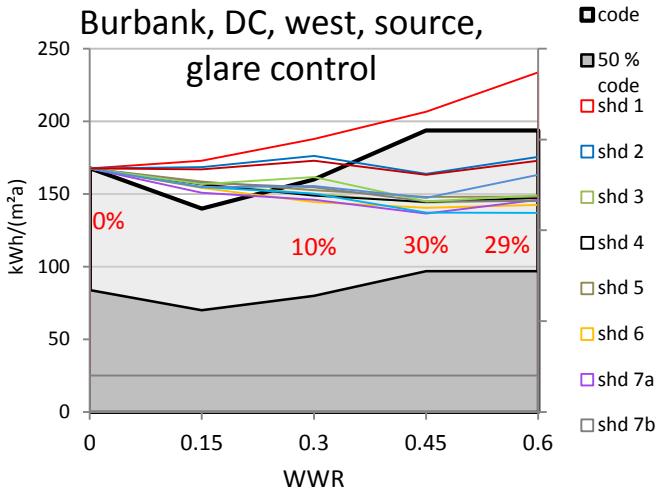

Figure 23b: Total source energy with daylighting control and with glare control in Burbank on a west facade.

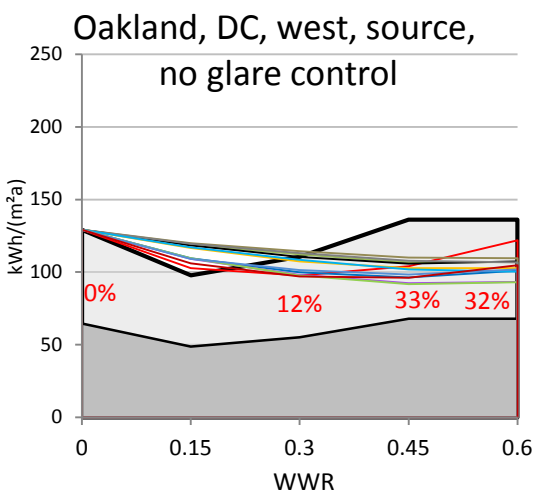

Figure 24a: Total source energy with daylighting control and without glare control in Oakland on a west facade.

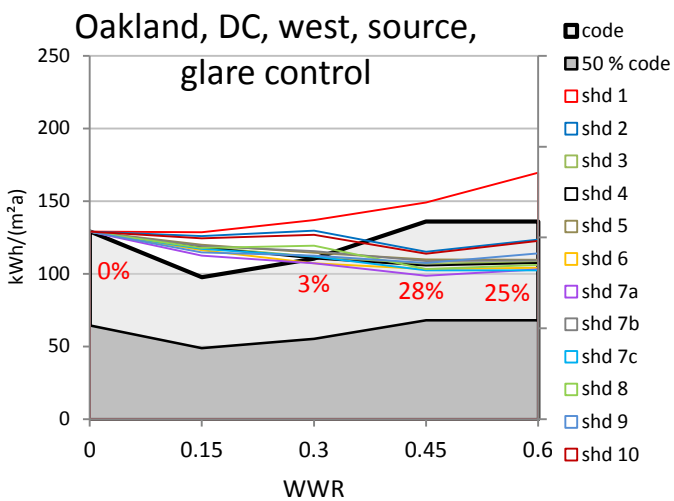

Figure 24b: Total source energy with daylighting control and with glare control in Oakland on a west façade.

The results for the west façade without glare control are similar to those on the east façade. When glare control is applied, the performance loss is less on the west façade than on the east facade because of the lower numbers of hours when the interior shade is down.

With glare control, all exterior shades except for shd 1, shd 2, shd 9 and shd 10 show a comparable energy performance with savings of 29-30 % in Burbank and 25-28 % in Oakland for WWRs > 45 %.

6. Discussion

The paper presents results of a simulation study where the geometry and material properties of twelve different exterior shading systems were investigated. For lighting energy, the prototypical large office building was modeled with and without daylighting controls. In Sections 4 and 5, an additional interior shade was modeled and deployed when a discomfort glare condition occurred. The impact of glare control through the interior shade on EUI was assessed.

Without daylighting controls and without interior shade, all exterior slat shading systems were beneficial for east, south, west and north orientation. While a low cut-off angle was always favorable for the cases without daylighting controls, for the case with daylighting controls, the admission of more daylight through a higher cut-off angle has a positive impact on the overall energy balance. For WWRs of 60 % and with daylighting controls, all geometries were beneficial, but there was an optimum at a moderate cut-off angle for the considered California climates and latitudes. For north orientation and smaller WWRs, higher cut-off angles are recommended over more closed shades when daylighting controls are installed. With daylighting controls, highly reflective surfaces are beneficial while the impact of surface reflectance was negligible for the considered shading systems when there was no daylighting control.

In perimeter zones, shades with high direct transmission lead to a significant number of hours with discomfort glare. In the simulation model with glare control, the interior shade was pulled down during glare conditions. Glare control through interior shades had no positive impact on overall energy use when used in combination with exterior shades, but in several cases it significantly increased energy use. The spread in performance amongst the twelve exterior shades was much larger when glare control was applied, i.e. the choice of the shading system highly impacted EUI. With glare control, the maximum energy savings that could be achieved with exterior shades were much less especially on the east façade, where the interior shades got pulled in the morning and stayed down for the remainder of the day. On the west façade, too, significant performance decreases were found with glare control. Changing the scenario of how long the interior shade stays down, may change the results for the East and South façade where discomfort glare related to direct sun light occurs earlier in the day. An automation of interior shade, e.g. pulling up the interior shade after a couple of hours when there is no more direct light, remains an option that may lead lower EUIs.

Despite the impact of glare control, the best performing shades did not show an increase in EUI with larger window-to-wall ratios when using daylighting controls. This is an important finding when entering the discussion about the optimum percentage of transparent area in a façade; a discussion in which architects, building engineers and owners often have different opinions about design aesthetics and expected energy cost.

7. Conclusions

The study showed that the paradigm of moderate window-to-wall ratios to reduce cooling load is questionable given the possible energy savings that can be achieved with a combination of exterior shades and daylighting controls. While the presented results assumed fixed exterior shades that were not controlled in any way, one can presume that adding shade automation will improve solar control and lead to even better performing buildings. One of the major tasks in the future will be to develop shades that correspond to design criteria, allow view to the outside while avoiding discomfort glare and fulfill all technical requirements to be used on high-rise buildings. If all of these requirements are met, there should be no more limitation with respect to window-to-wall ratio.

The significant impact of glare control on energy use intensity should encourage the building science community to put more focus on the occurrence of discomfort glare. The possibility of discomfort glare in offices, especially on computer work stations, is a highly neglected issue in real buildings. Even in new constructions with exterior shades, retrofits with interior shades are frequently necessary for this reason. When using exterior shades to reduce solar load, special attention should be given to the choice of the exterior shade:

some of the investigated, commercially available exterior shades performed very well for glare control while others did not.

Another conclusion that can be drawn from the presented results is that glare control needs to be modeled when running building energy simulations to predict future energy use. Without modeling the fact that occupants will deploy an interior shade when light impedes their ability to work, simulation results overestimate the energy savings that can be achieved. Occupant behavior highly influences the energy use in a building - in the simulation as well as in real buildings - and the simulation community will have to take this into the account in future developments.

Acknowledgments

This work was supported by the California Energy Commission through its Public Interest Energy Research (PIER) Program on behalf of the citizens of California.

Completion of the paper was supported through the research center High Performance Composite Constructions, HiPerCon, at University of Kaiserslautern.

References

[1] NFRC 200-2010: Procedure for Determining Fenestration Product Solar Heat Gain Coefficient and Visible Transmittance at Normal Incidence. National Fenestration Rating Council, Inc.

[2] EN 13363-2:2005: Solar protection devices combined with glazing - Calculation of total solar energy transmittance and light transmittance - Part 2: Detailed calculation method

[3] 2013 Nonresidential Compliance Manual for the 2013 Building Energy Efficiency Standards. Title 24, Part 6, and associated. CEC-400-2013-002-CMF. California Energy Commission, Edmund G. Brown Jr., Governor

[4] ISO 15099-2003. Thermal Performance of Windows, Doors and Shading Devices—Detailed Calculations. Geneva: International Organization for Standardization

[5] http://smartlouvre.com/ (accessed June 22, 2015).

[6] http://www.clauss-markisen.de/ (accessed June 22, 2015).

[7] https://www.warema.de/PRIVATKUNDEN/PRODUKTE/Raffstoren/Abdunkelungs_Raffstoren.php (accessed June 22, 2015).

[8] http://www.okalux.de/loesungen/marken/okatech/ (accessed June 22, 2015).

[9] http://en.sergeferrari.com/bioclimatic-facade/a-facade-for-a-new-style-of-architecture/ (accessed June 22, 2015).

[10] McNeil, A.; Jonsson, C.J.; Appelfeld, D.; Ward, G.; Lee, E.S.: A validation of a ray-tracing tool used to generate bi-directional scattering distribution functions for complex fenestration systems. Solar Energy. Volume 98, Part C, December 2013, Pages 404-414

[11] Grobe, L. O.; Wittkopf, S. ; Apian-Bennewitz, P. J.; Jonsson C.; Rubin, M.: Experimental validation of bidirectional reflection and transmission distribution measurements of specular and scattering materials, Proc. SPIE 7725, 772510 (2010); doi:10.1117/12.854011

[12] Mitchell, R.; Kohler, D.; Klems, J.; Rubin, M.; Arasteh, D.; Huizenga, C.; Yu, T.; Curcija, D. (editors): Window 6.2/ Therm 6.2 Research Version User Manual, Berkeley, CA, 2008. LBNL-941. Available at: http://windows.lbl.gov/software/window/window.html (accessed June 22, 2015).

[13] EnergyPlus InputOutputReference.pdf, Release V8.1.08, download available: http://apps1.eere.energy.gov/buildings/energyplus/pdfs/inputoutputreference.pdf (accessed June 22, 2015).

[14] EIA. (2005). 2003 Commercial Buildings Energy Consumption Survey. Washington, DC: Energy Information Administration. http://www.eia.gov/consumption/commercial/index.cfm (accessed June 22, 2015).
[15] http://www.energycodes.gov/development/commercial/90.1_models (accessed June 22, 2015).
[16] http://bees.archenergy.com/referencemethod.html (accessed June 22, 2015).
[17] Klems, J H.: A New Method for Predicting the Solar Heat Gain of Complex Fenestration Systems – I. Overview and Derivation of the Matrix Layer Calculation. ASHRAE Transactions 100 (1), 1994.
[18] Klems, J H.: A New Method for Predicting the Solar Heat Gain of Complex Fenestration Systems – II. Detailed Description of the Matrix Layer Calculation. University of California: ASHRAE Transactions 100 (1), 1994.
[19] Winkelmann, F.C.: Modeling Windows in EnergyPlus. Seventh International IBPSA Conference. Rio de Janeiro, Brazil, August 13-15, 2001.
[20] http://radsite.lbl.gov/radiance/ (accessed June 22, 2015).
[21] McNeil, A.; Lee, E.S.: A validation of the Radiance three-phase simulation method for modeling annual daylight performance of optically-complex fenestration systems. Journal of Building Performance Simulation 2012: 1-14
[22] Zuo, W.; McNeil, A.; Wetter, M.; Lee, E.S.: Acceleration of the matrix multiplication of Radiance three phase daylighting simulations with parallel computing on heterogeneous hardware of personal computer. Journal of Building Performance Simulation, 2013.
[23] Fernandes, L.; Lee, E.S.; McNeil, A.; Jonsson, J.C.; Nouidui, T.S.; Pang, X.; Hoffmann, S.: Angular selective window systems: Assessment of technical potential for energy saving, submitted to: Energy and Buildings, May 2014
[24] http://www.eia.gov/consumption/commercial/data/archive/cbecs/cbecs2003/lighting/lighting1.html (accessed June 22, 2015).
[25] Wienold, Jan. Daylight Glare in Offices. Fraunhofer Verlag, 2010. ISBN 978-3-8396-0162-4
[26] Clear, R.D.: Discomfort Glare: What do we actually know? Lawrence Berkeley National Laboratory Windows and Envelope Materials Group Building Technology and Urban Systems Department. Lighting Research and Technology, 19 April 2012. Available at: http://btech.lbl.gov/sites/all/files/5584_0.pdf (accessed June 22, 2015).

Appendix A: Geometry of building prototype

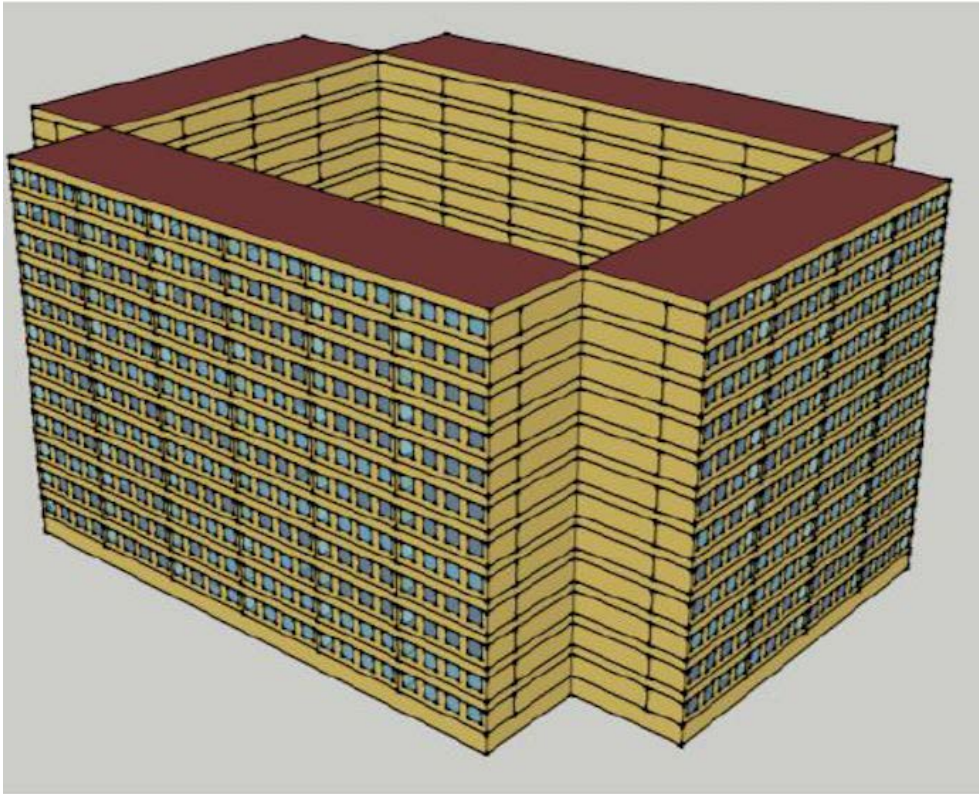

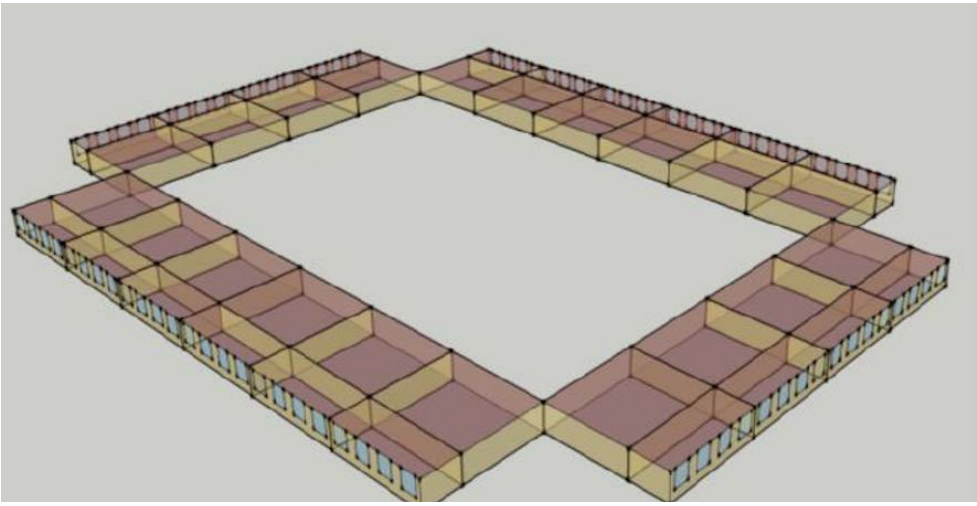

Appendix B: Geometry of exterior shades

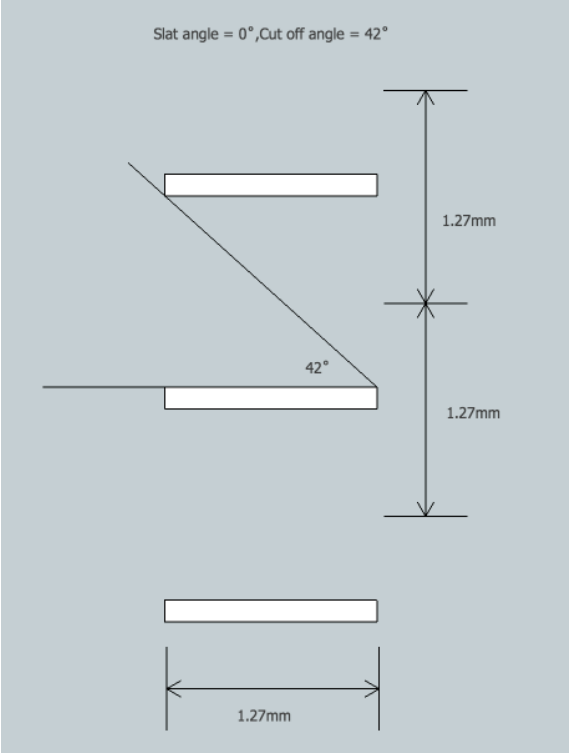

shd 1

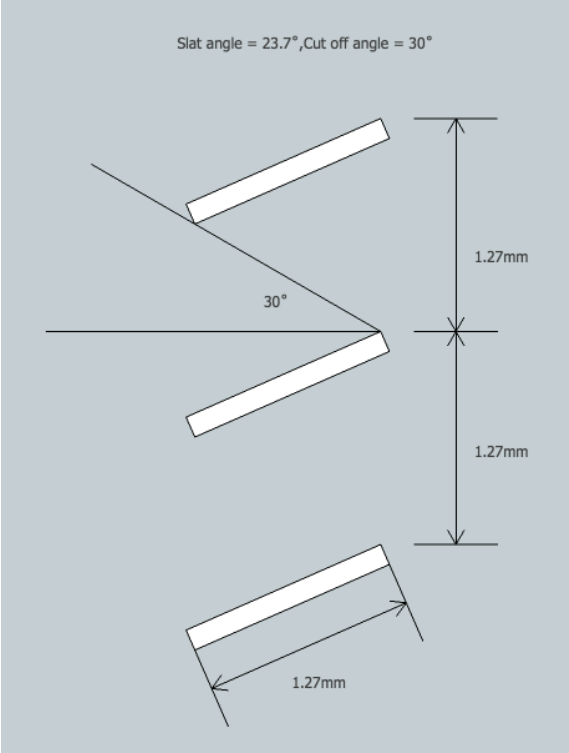

shd 2

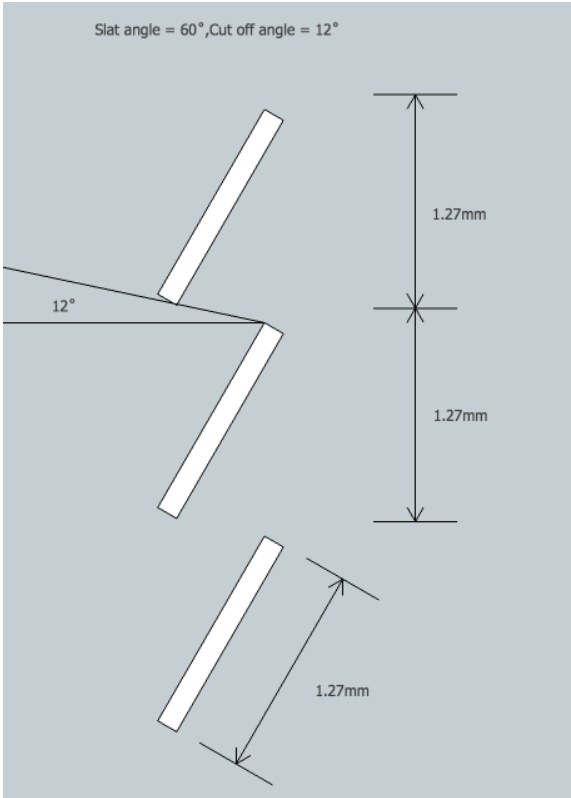

shd 3

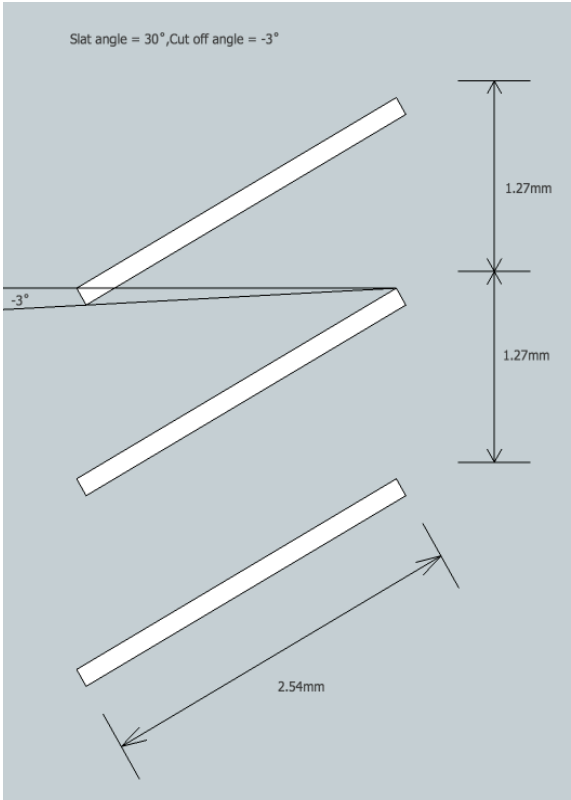

shd 4

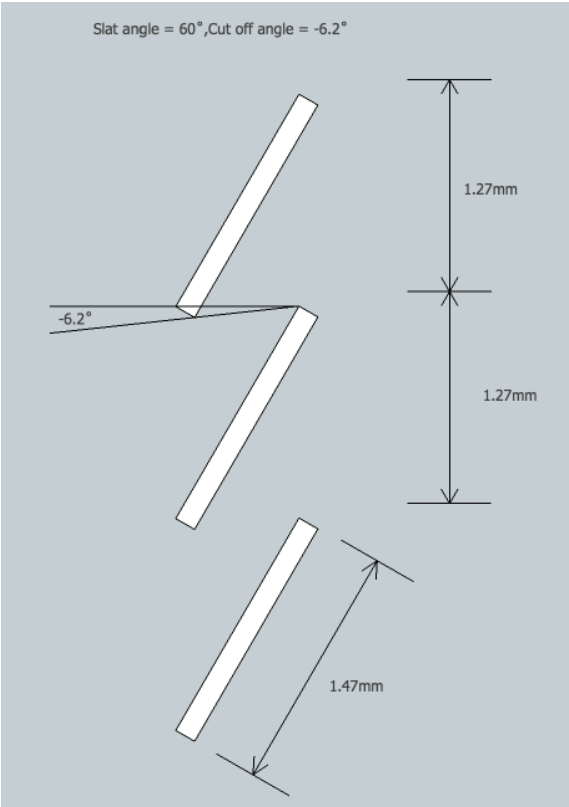

shd 5

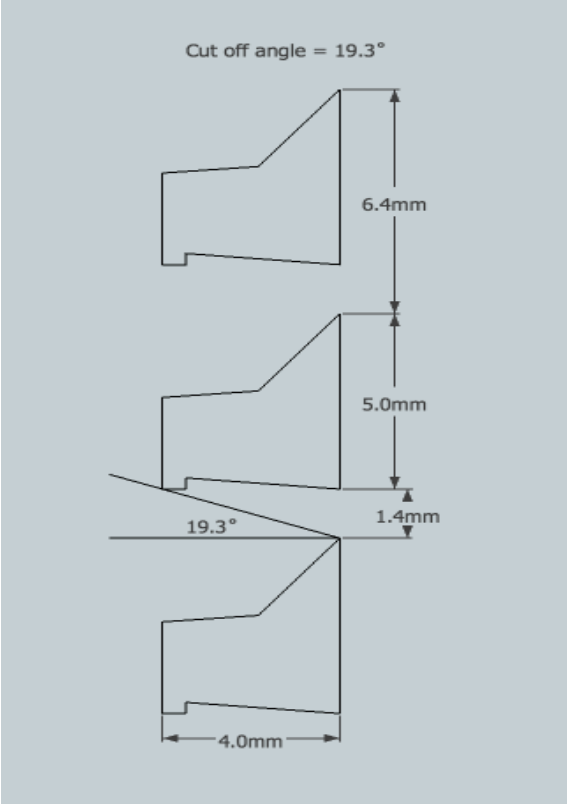

shd 6

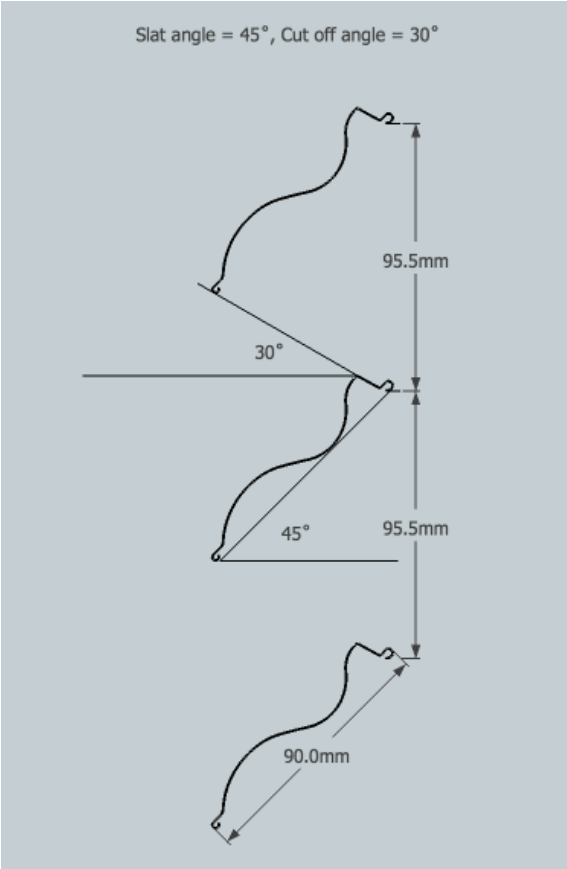

shd 7[7]

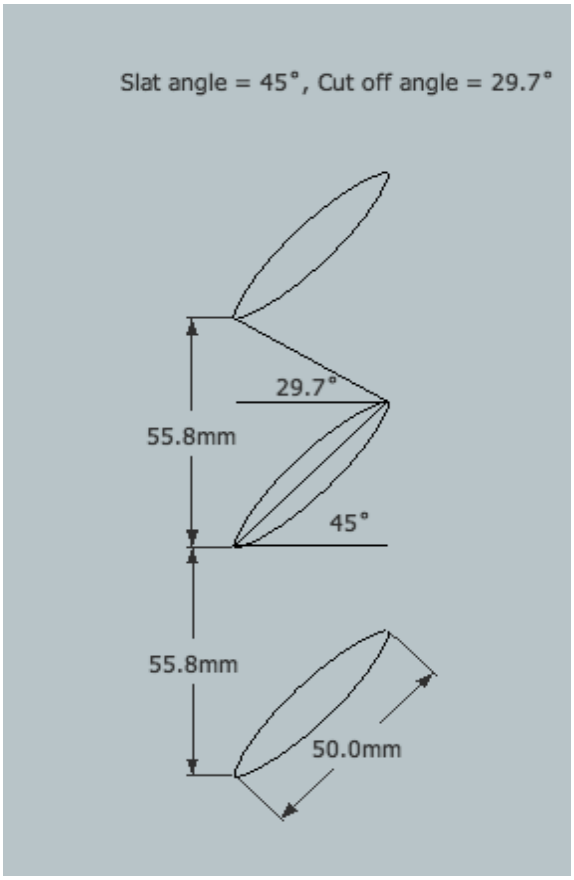

shd 8

[7] The commercial product differs from the drawing: the slat spacing is only 83 mm so that the shade can be fully closed.